

## Histone Deacetylase 7 Controls Endothelial Cell Growth Through Modulation of $\beta$ -Catenin

Andriana Margariti, Anna Zampetaki, Qingzhong Xiao, Boda Zhou, Eirini Karamariti, Daniel Martin, Xiaoke Yin, Manuel Mayr, Hongling Li, Zhongyi Zhang, Elena De Falco, Yanhua Hu, Gillian Cockerill, Qingbo Xu and Lingfang Zeng

*Circ. Res.* 2010;106;1202-1211; originally published online Mar 11, 2010;

DOI: 10.1161/CIRCRESAHA.109.213165

Circulation Research is published by the American Heart Association, 7272 Greenville Avenue, Dallas, TX 75214

Copyright © 2010 American Heart Association. All rights reserved. Print ISSN: 0009-7330. Online ISSN: 1524-4571

The online version of this article, along with updated information and services, is located on the World Wide Web at:

<http://circres.ahajournals.org/cgi/content/full/106/7/1202>

Data Supplement (unedited) at:

<http://circres.ahajournals.org/cgi/content/full/CIRCRESAHA.109.213165/DC1>

Subscriptions: Information about subscribing to Circulation Research is online at  
<http://circres.ahajournals.org/subscriptions/>

Permissions: Permissions & Rights Desk, Lippincott Williams & Wilkins, a division of Wolters Kluwer Health, 351 West Camden Street, Baltimore, MD 21202-2436. Phone: 410-528-4050. Fax: 410-528-8550. E-mail:  
[journalpermissions@lww.com](mailto:journalpermissions@lww.com)

Reprints: Information about reprints can be found online at  
<http://www.lww.com/reprints>

## Histone Deacetylase 7 Controls Endothelial Cell Growth Through Modulation of $\beta$ -Catenin

Andriana Margariti, Anna Zampetaki, Qingzhong Xiao, Boda Zhou, Eirini Karamariti, Daniel Martin, Xiaoke Yin, Manuel Mayr, Hongling Li, Zhongyi Zhang, Elena De Falco, Yanhua Hu, Gillian Cockerill, Qingbo Xu, Lingfang Zeng

**Rationale:** Histone deacetylase (HDAC)7 is expressed in the early stages of embryonic development and may play a role in endothelial function.

**Objective:** This study aimed to investigate the role of HDAC7 in endothelial cell (EC) proliferation and growth and the underlying mechanism.

**Methods and Results:** Overexpression of HDAC7 by adenoviral gene transfer suppressed human umbilical vein endothelial cell (HUVEC) proliferation by preventing nuclear translocation of  $\beta$ -catenin and downregulation of T-cell factor-1/Id2 (inhibitor of DNA binding 2) and cyclin D1, leading to G<sub>1</sub> phase elongation. Further assays with the TOPFLASH reporter and quantitative RT-PCR for other  $\beta$ -catenin target genes such as Axin2 confirmed that overexpression of HDAC7 decreased  $\beta$ -catenin activity. Knockdown of HDAC7 by lentiviral short hairpin RNA transfer induced  $\beta$ -catenin nuclear translocation but downregulated cyclin D1, cyclin E1 and E2F2, causing HUVEC hypertrophy. Immunoprecipitation assay and mass spectrometry analysis revealed that HDAC7 directly binds to  $\beta$ -catenin and forms a complex with 14-3-3  $\epsilon$ ,  $\zeta$ , and  $\eta$  proteins. Vascular endothelial growth factor treatment induced HDAC7 degradation via PLC $\gamma$ -IP3K (phospholipase C $\gamma$ -inositol-1,4,5-trisphosphate kinase) signal pathway and partially rescued HDAC7-mediated suppression of proliferation. Moreover, vascular endothelial growth factor stimulation suppressed the binding of HDAC7 with  $\beta$ -catenin, disrupting the complex and releasing  $\beta$ -catenin to translocate into the nucleus.

**Conclusions:** These findings demonstrate that HDAC7 interacts with  $\beta$ -catenin keeping ECs in a low proliferation stage and provides a novel insight into the mechanism of HDAC7-mediated signal pathways leading to endothelial growth. (*Circ Res.* 2010;106:1202-1211.)

**Key Words:** HDAC7 ■  $\beta$ -catenin ■ VEGF ■ 14-3-3 ■ cell cycle

Endothelial cells (ECs) are critical cellular components of blood vessels and act as selectively permeable barriers between blood and tissues. In standard physiological conditions they are compact,<sup>1</sup> growth inhibited, protected from apoptosis and retain full control of permeability.<sup>2,3</sup> In contrast, following injury, they become elongated, highly motile, and stimulate cell replication and replacement in response to growth factors.<sup>4</sup>

Adherens junctions are formed by vascular endothelial (VE)-cadherin. VE-cadherin predominantly mediates cell contact and regulates angiogenesis by controlling EC adhesion, migration, proliferation, and survival via interactions with vascular endothelial growth factor (VEGF) receptors.<sup>5,6</sup>

VEGF is involved in new vessel formation during embryogenesis and in proliferative diseases in adults by inducing

differentiation in vascular structures and EC proliferation.<sup>7</sup> A number of signal transduction molecules are activated or modified in response to VEGF stimulation, such as phosphoinositide 3-kinase (PI 3-kinase) and its downstream substrates, serine/threonine kinase Akt/protein kinase B, phospholipase (PL)C $\gamma$ , Src family tyrosine kinases, the Ras GTPase-activating protein, small adaptor molecule Nck, focal adhesion kinase C, extracellular signal-regulated kinase (ERK), and p38 mitogen-activated protein kinase.<sup>8,9</sup>

$\beta$ -Catenin is a signaling molecule that promotes cell proliferation and growth by inducing gene transcription through activation of T-cell factor/lymphoid enhancer factor (TCF/LEF),<sup>10</sup> Id2 (inhibitor of DNA binding 2),<sup>11</sup> and follistatin<sup>12</sup> transcription factors. The phosphorylation of  $\beta$ -catenin by casein kinase 1 (CK1) at Ser45 and by glycogen

Original received May 20, 2009; resubmission received November 13, 2009; revised resubmission received February 26, 2010; accepted February 26, 2010.

From the Cardiovascular Division (A.M., A.Z., Q.X., E.K., D.M., X.Y., M.M., H.L., Z.Z., E.D.F., Y.H., Q.X., L.Z.), King's College London British Heart Foundation Centre, London, United Kingdom; Department of Physiology and Pathophysiology (B.Z.), Peking University, China; and Department of Cardiovascular Medicine (G.C.), St. George's University of London, United Kingdom.

Correspondence to Dr Lingfang Zeng, Cardiovascular Division, King's College London, The James Black Centre, 125 Coldharbour Lane, London SE5 9NU, United Kingdom. E-mail [Lingfang.zeng@kcl.ac.uk](mailto:Lingfang.zeng@kcl.ac.uk)

© 2010 American Heart Association, Inc.

*Circulation Research* is available at <http://circres.ahajournals.org>

DOI: 10.1161/CIRCRESAHA.109.213165

synthase kinase 3 (GSK3) at Thr41, Ser37, and Ser33, targets  $\beta$ -catenin for ubiquitination and degradation through the proteasome. Mitogenic factors promote  $\beta$ -catenin signaling through inhibition of GSK3. This reduces the phosphorylation of  $\beta$ -catenin and increases its nuclear accumulation where it stimulates TCF/LEF-dependent gene transcription.<sup>13</sup> Therefore, the stability and/or subcellular localization of  $\beta$ -catenin can be affected by multiple signaling events. However, there is not sufficient information to fully explain how the stabilization and cytoplasmic-nuclear translocation of  $\beta$ -catenin are regulated.

Histone deacetylases (HDACs) regulate several biological processes such as cell-cycle, cell differentiation and survival.<sup>14–17</sup> Histone deacetylase (HDAC)7 is a member of the class II HDACs and is expressed in the vascular endothelium during early embryogenesis where it maintains vascular integrity.<sup>18</sup> Silencing of HDAC7 in ECs alters their morphology and motility and prevents their assembly into tube-like structures.<sup>19</sup> Furthermore, VEGF induces HDAC, and in particular HDAC7 phosphorylation. The responsive phosphorylation sites in HDAC7 are critical for VEGF-induced EC proliferation.<sup>20,21</sup> Therefore, HDAC7 is critical during angiogenesis and mainly functions as a transcriptional repressor for genes such as membrane type 1 metalloprotease and matrix metalloproteinase-10.<sup>20</sup> However, the detailed mechanisms of how HDAC7 is involved in these key angiogenic processes is still unclear. In this study we demonstrate that HDAC7 controls EC growth through modulation of  $\beta$ -catenin and maintains ECs in a low proliferation stage.

Non-standard Abbreviations and Acronyms	
Ad-HD7	HDAC7 adenovirus
Ad-tTA	tetracycline-controlled transactivator tTA adenovirus
BrdUrd	bromodeoxyuridine
HA	hemagglutinin
HDAC	histone deacetylase
HUVEC	human umbilical vein endothelial cell
Id2	inhibitor of DNA binding 2
IP3	inositol-1,4,5-trisphosphate
IP3K	inositol-1,4,5-trisphosphate kinase
LEF	lymphoid enhancer factor
moi	multiplicity of infection
MTT	3-(4,5-dimethylthiazol-2-yl)-2,5-diphenyl tetrazolium bromide
PLC	phospholipase C
Rb	retinoblastoma
shRNA	short hairpin RNA
VE	vascular endothelial
VEGF	vascular endothelial growth factor

### Methods

An expanded Methods section is available in the Online Data Supplement at <http://circres.ahajournals.org>.

### Cell Culture

Human umbilical vein endothelial cells (HUVECs) were isolated from the human umbilical cord and cultured on collagen I-coated

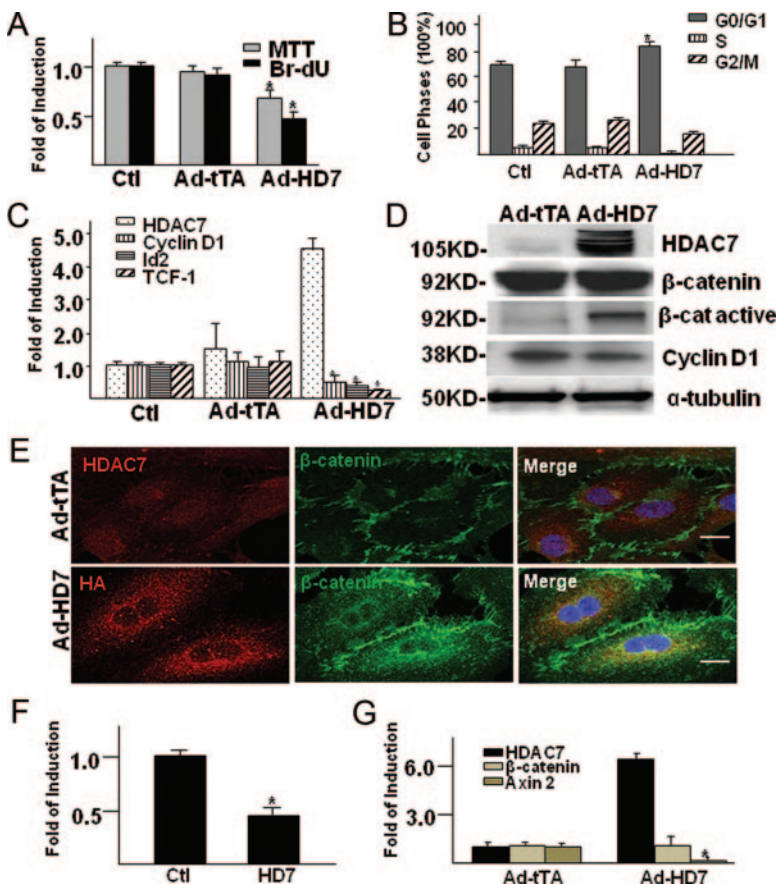


**Figure 1. Elevated HDAC7 suppresses EC proliferation via prevention of  $\beta$ -catenin translocation.** **A**, Overexpression of HDAC7 decreases metabolism (MTT) and BrdUrd incorporation. HUVECs were uninfected (Ctl) or infected with Ad-HD7 or Ad-tTA. MTT and BrdUrd assays were performed 48 hours after infection. \* $P < 0.05$ . **B**, Fluorescence-activated cell-sorting analysis revealed that overexpression of HDAC7 in HUVECs prevents the G<sub>1</sub>/S phase transition. **C and D**, Overexpression of HDAC7 decreases cyclin D1, Id2, and TCF-1 expression at the RNA level by real-time PCR (\* $P < 0.05$ ) (**C**) or at the protein level by Western blot (**D**) 48 hours after infection.  $\alpha$ -Tubulin was included as loading control. Overexpression of HDAC7 increases active  $\beta$ -catenin levels but decreases its target gene expression, Id2 and TCF-1. **E**, HDAC7 overexpression retains  $\beta$ -catenin in the cytoplasm. Double immunofluorescence staining was performed 48 hours after infection. Exogenous HDAC7 was revealed by anti-HA antibody. DAPI was used to stain the cell nucleus (bar, 100  $\mu$ m). **F and G**, TOP-FLASH reporter gene assay (**F**) and real-time PCR for Axin2 (**G**) confirmed that overexpression of HDAC7 decreases  $\beta$ -catenin activity.

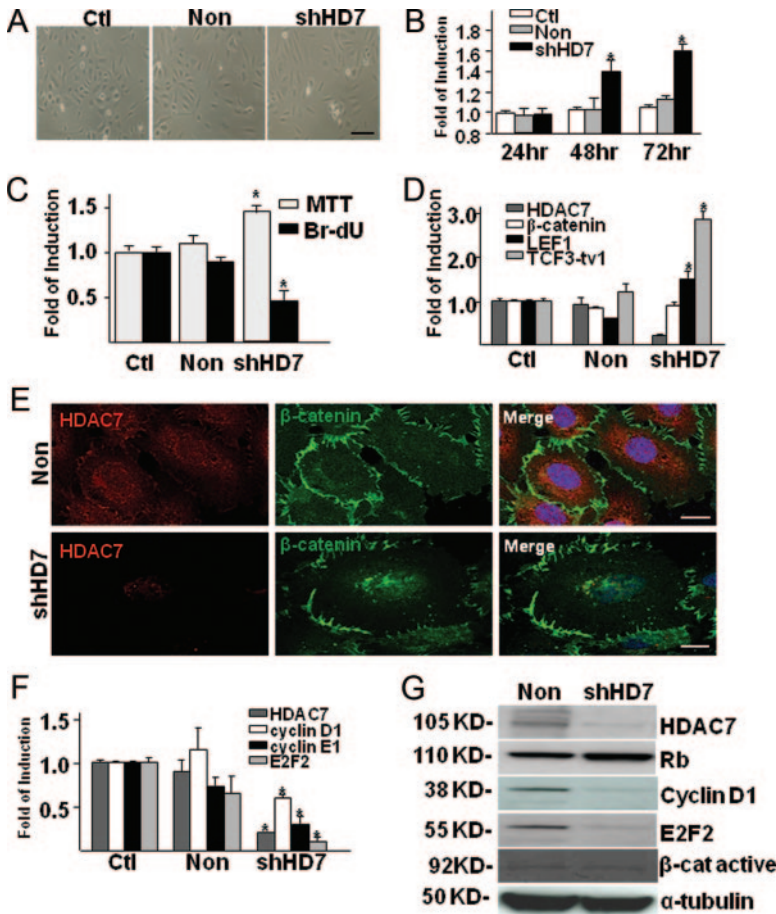


**Figure 2. Knockdown of HDAC7 causes EC hypertrophy.** **A**, HUVECs were uninfected (Ctl) or infected with nontarget (Non) or HDAC7 (shHD7) shRNA. Knockdown of HDAC7 increases cell size 72 hours after infection (bar, 50  $\mu$ m). **B**, Knockdown of HDAC7 increases HUVEC size as revealed by cell size calculation at 24, 48, and 72 hours after infection using Beckman Coulter. Uninfected (Ctl) and nontarget shRNA (Non) were included as controls. \* $P$ <0.05. **C**, Knockdown of HDAC7 increases metabolism (MTT) but decreases BrdUrd incorporation, 72 hours after infection. \* $P$ <0.05. **D**, The expression of  $\beta$ -catenin target genes was increased by knockdown of HDAC7. Real-time PCR was performed at 72 hours after infection. \* $P$ <0.05. **E**, Knockdown of HDAC7 increases  $\beta$ -catenin localization in nucleus. Double-immunofluorescence staining was performed 72 hours after infection with shRNA lentiviral particles (bar, 100  $\mu$ m). **F**, Knockdown of HDAC7 decreases cyclin D1, E1, and E2F2 expression. Real-time PCR was performed at 72 hours after infection. \* $P$ <0.05. **G**, The expression of Rb, cyclin D1, and E2F2, and  $\beta$ -catenin active proteins was evaluated by Western blot analysis.

flasks in EGM-2 medium (Clonetics) or in M199 medium supplemented with 1 ng/mL  $\beta$ -EC growth factor (SIGMA), 3  $\mu$ g/mL EC Growth Supplement from bovine neural tissue (Sigma), 10 U/mL heparin, 1.25  $\mu$ g/mL thymidine, 5% FBS (PAA, A15-108),<sup>22</sup> and 100  $\mu$ g/mL penicillin and streptomycin.

**Ad-Virus Construction**

The Ad-HDAC7 viral DNA (Ad-HD7) was constructed as described previously.<sup>23</sup>

**Results**

**Elevated HDAC7 Suppresses EC Proliferation via Prevention of  $\beta$ -Catenin Translocation**

To explore the function of HDAC7 in the maintenance of EC homeostasis, we first studied the effect of HDAC7 overexpression by adenoviral gene transfer (Ad-HD7) on HUVEC proliferation. Overexpression of HDAC7 did not alter HUVEC morphology (Online Figure I, A and B); however, the growth rate of HUVECs decreased. Ad-HD7-infected cells required longer to reach confluence as compared to uninfected or tetracycline-controlled transactivator tTA adenovirus (Ad-tTA)-infected cells, as revealed by a decrease in 3-(4,5-dimethylthiazol-2-yl)-2,5-diphenyl tetrazolium bromide (MTT)-based mitochondrial enzyme activity, BrdUrd incorporation assays (Figure 1A), and cell number counting (Online Figure I, C). No increases in apoptosis and caspase activation were detected in Ad-HD7-infected cells (Online Figure II, A and B). Furthermore fluorescence-activated cell-sorting analysis demonstrated that overexpression of

HDAC7 in HUVECs prevented the G1/S phase transition (Figure 1B). The  $\beta$ -catenin pathway plays an important role in EC growth and G<sub>1</sub>/S phase transition. We wondered whether HDAC7 suppressed EC proliferation through modulation of this pathway. To test this we examined the effect of HDAC7 overexpression on  $\beta$ -catenin target gene expression. As shown in Figure 1C, cyclin D1, Id2, and TCF-1 mRNAs were significantly decreased in Ad-HD7-infected HUVECs. The decrease of cyclin D1 was further confirmed by Western blot (Figure 1D). The mRNA (Figure 1G) and protein levels (Figure 1D) of  $\beta$ -catenin itself did not change in Ad-HD7-infected cells as compared to control virus-infected cells. Actually, the active form of  $\beta$ -catenin was increased in Ad-HD7-infected cells (Figure 1D). Therefore, the decrease in the expression of these genes might be attributable to reduced nuclear localization of  $\beta$ -catenin. Double immunofluorescence staining revealed that in uninfected or Ad-tTA virus-infected HUVECs,  $\beta$ -catenin was exclusively located in the pericellular junctions (Figure 1E, top) in confluent cells. Most subconfluent cells showed similar  $\beta$ -catenin staining with only a few cells showing nuclear localization (Online Figure I, D). In contrast, in Ad-HD7-infected cells,  $\beta$ -catenin localized to both the pericellular junctions and the cytoplasm. Very little staining was observed in the nucleus (Figure 1E, bottom). There was a strong colocalization of  $\beta$ -catenin and HDAC7 in the cytoplasm. This observation was confirmed by other experiments described later. Further assays with the TOPFLASH reporter (Figure 1F) and quantitative RT-PCR

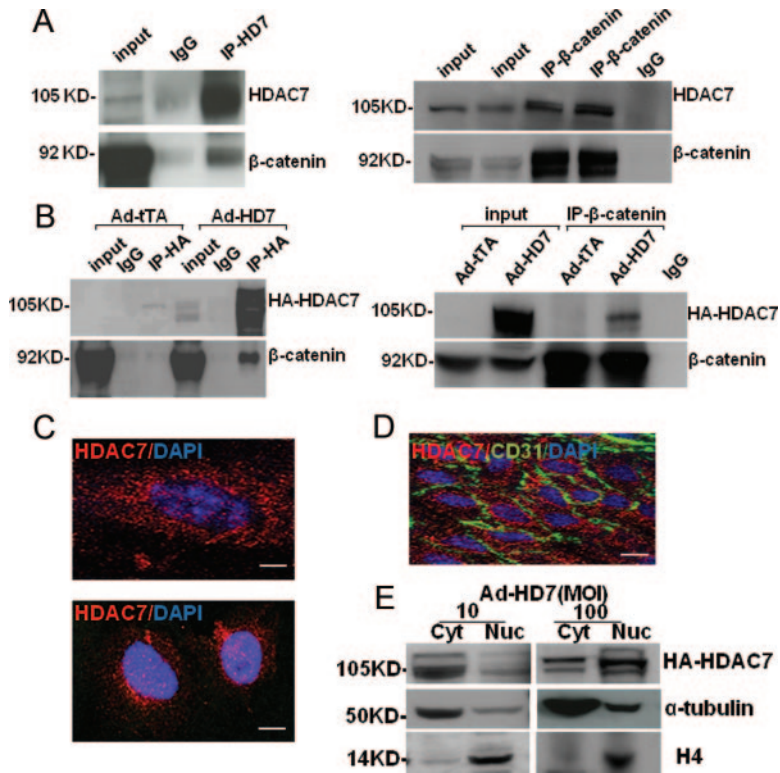


**Figure 3. HDAC7 binds to  $\beta$ -catenin.** **A and B,** Coimmunoprecipitation assays show the direct binding of  $\beta$ -catenin to endogenous HDAC7 (**A**; left, immunoprecipitation [IP] with HDAC7; right, immunoprecipitation with  $\beta$ -catenin) and exogenous HDAC7 (**B**; left, immunoprecipitation with HA; right, immunoprecipitation with  $\beta$ -catenin). **C,** Immunostaining shows the different localization pattern of HDAC7 in different cells. **Top,** Cytoplasmic localization of HDAC7 in the majority of cells. **Bottom,** Nuclear localization of HDAC7 in a small portion of the cells. **Bar,** 100  $\mu$ m. **D,** En face staining of arteries obtained from wild-type mice showed that HDAC7 is predominantly expressed in the cytoplasm. Double staining of HDAC7 (**red**) and CD31 (**green**) defined the endothelium monolayer in these samples. **Bar,** 50  $\mu$ m. **E,** Western blots show that HDAC7 localization occurs in a multiplicity of infection-dependent manner. HUVECs were infected with 10 or 100 MOI. HDAC7 localization was detected by cellular fractionation and Western blot 48 hours after infection.  $\alpha$ -Tubulin and H4 were included as loading controls for cytoplasmic and nuclear fractions, respectively. High multiplicities of infection of Ad-HD7 virus infection increases HDAC7 nuclear localization.

for other  $\beta$ -catenin target genes such as Axin2 (Figure 1G) confirmed that overexpression of HDAC7 decreased  $\beta$ -catenin activity. These results suggest that overexpression of HDAC7 suppresses EC proliferation through retention of  $\beta$ -catenin in the cytoplasm and downregulation of cyclin D1.

### Knockdown of HDAC7 Causes EC Hypertrophy

Because overexpression of HDAC7 suppressed EC proliferation, we hypothesized that downregulation of HDAC7 could increase EC proliferation. To test this, we knocked down HDAC7 mRNA via short hairpin (sh)RNA lentiviral particles. Downregulation of HDAC7 mRNA did not affect the expression of other HDACs (Online Figure III, A). Knockdown of HDAC7 resulted in enlarged cells as compared to uninfected or nontargeting shRNA lentivirus-infected cells (Figure 2A). Calculation of the cell size confirmed that HDAC7 shRNA lentivirus-infected cells were significantly larger (Figure 2B). Furthermore, knockdown of HDAC7 increased MTT-based mitochondrial enzyme activity, but surprisingly BrdUrd incorporation (Figure 2C) and cell counts (online Figure III, B) were decreased. In contrast to the overexpression data, knockdown of HDAC7 upregulated LEF1 and TCF3-tv1 expression (Figure 2D). In concert with this, translocation of  $\beta$ -catenin to the nucleus was enhanced by knockdown of HDAC7 (Figure 2E). H3 nuclear staining was included as a positive control and is shown in Online Figure IV. However, knockdown of HDAC7 downregulated cyclin D1 and E1 mRNA (Figure 2F) and protein (Figure 2G) expression, but increased retinoblastoma (Rb) protein (Figure 2G). This leads to downregulation of E2F2 expression, whereas the  $\beta$ -catenin active form did not change (Figure 2F and 2G). These results suggest that HDAC7 deficiency

induces EC hypertrophy by increasing  $\beta$ -catenin translocation via modulation of the cyclins/Rb pathway.

### HDAC7 Binds to $\beta$ -Catenin

We hypothesized that HDAC7 and  $\beta$ -catenin may interact directly. Coimmunoprecipitation experiments were performed to test this hypothesis. Indeed, direct binding of  $\beta$ -catenin to endogenous HDAC7 (Figure 3A; left, IP with HDAC7; right, IP with  $\beta$ -catenin) and exogenous HDAC7 (Figure 3B; left, IP with hemagglutinin [HA]; right, IP with  $\beta$ -catenin) was observed. HDAC7 is a shuttle protein and traffics between the cytoplasm and the nucleus. To identify the localization of HDAC7 in our culture conditions, immunofluorescence staining for endogenous HDAC7 was performed. HDAC7 predominantly localized to the cytoplasm in HUVECs (Figure 3C, top). HDAC7 was only localized to the nucleus in a small portion of the cells (Figure 3C, top). A similar phenomenon was observed in intact ECs in vivo. En face staining of arteries obtained from wild type mice showed that HDAC7 is predominantly expressed in the cytoplasm (Figure 3D). In vitro, in our overexpression system the localization of HDAC7 was multiplicity of infection (moi)-dependent. Specifically, HDAC7 mainly localized to the cytoplasm at low multiplicities of infection, such as 10 MOI (Figure 3E). However, at high multiplicities of infection (eg, 100 MOI), HDAC7 predominantly localized to the nucleus (Figure 3E). These data indicate that HDAC7 is mainly expressed in the cytoplasm under physiological conditions.

### HDAC7 Links 14-3-3 $\epsilon$ , $\zeta$ , $\eta$ Proteins and $\beta$ -Catenin to Form a Complex

To better understand how HDAC7 regulates the stabilization and translocation of  $\beta$ -catenin, HDAC7-associated

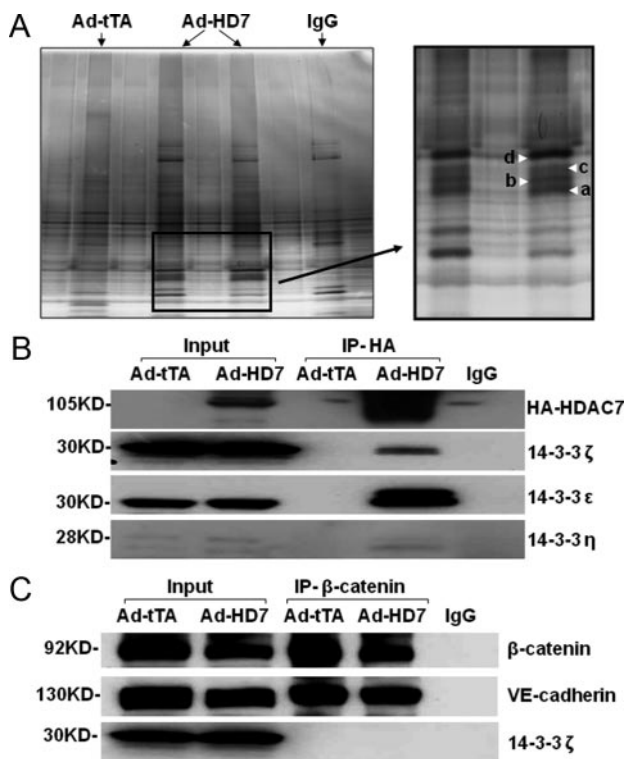


**Figure 4. HDAC7 links 14-3-3  $\epsilon$ ,  $\zeta$ , and  $\eta$  proteins and  $\beta$ -catenin to form a complex. **A**, Silver staining shows the HDAC7 associated proteins. HUVECs were infected with Ad-tTA- or Ad-HD7- and HDAC7-associated proteins were pulled down by anti-HA antibody and observed by silver staining (left). Right, Enlarged image. Bands a, b, c, and d were identified as 14-3-3  $\epsilon$ ,  $\zeta$ , and  $\eta$  by mass spectrometry. **B**, Coimmunoprecipitation assays confirmed the binding of HDAC7 with the 14-3-3 isoforms in HUVECs. **C**,  $\beta$ -Catenin bound to VE-cadherin but not to 14-3-3  $\zeta$ .**

proteins were isolated and analyzed by mass spectrometry in Ad-HD7-infected HUVECs as compared to control virus-infected cells (Figure 4A; Online Table II). The 14-3-3  $\epsilon$ ,  $\zeta$ , and  $\eta$  proteins were pulled down by HA antibody in Ad-HD7 infected cells. These results were further confirmed by coimmunoprecipitation assays (Figure 4B). Stabilization of  $\beta$ -catenin in the cytoplasm is regulated by the 14-3-3  $\zeta$  isoform.<sup>24</sup> We hypothesized that the 14-3-3 isoforms might bind directly to  $\beta$ -catenin or indirectly through HDAC7. Coimmunoprecipitation with anti- $\beta$ -catenin antibody could not detect the binding of the 14-3-3  $\zeta$  isoform, despite the association of  $\beta$ -catenin with VE-cadherin being detected (Figure 4C). This was also true with the 14-3-3  $\epsilon$ , and  $\eta$  isoforms (data not shown). Coimmunoprecipitation with 14-3-3  $\zeta$  was also performed and confirmed the above findings (Online Figure V). These results suggest that the 14-3-3 proteins may indirectly associate with  $\beta$ -catenin and that HDAC7 may act as a scaffold or docking site that stabilizes the complex and retains  $\beta$ -catenin in the cytoplasm.

#### VEGF Induces HDAC7 Protein Degradation Through the PLC $\gamma$ -IP3 Kinase Pathway

VEGF is a well-known mitogenic growth factor for ECs that modulates the VE-cadherin- $\beta$ -catenin complex and nuclear

translocation of  $\beta$ -catenin. We showed that HDAC7 bound and retained  $\beta$ -catenin in the cytoplasm. Thus, we postulated that crosstalk between VEGF signaling and HDAC7 may occur. First we detected the protein level of HDAC7 in VEGF-treated HUVECs by Western blot analysis. VEGF treatment rapidly decreased endogenous HDAC7 protein expression within 5 to 10 minutes via protein degradation (Figure 5A). Furthermore VEGF treatment suppressed the transcription of HDAC7 as demonstrated by luciferase reporter assays (Online Figure VI, A) and conventional and quantitative RT-PCR (Figure Online VI, B and C).

VEGF binding to its receptors can trigger multiple signal pathways. Selective inhibitors were used to distinguish the signaling pathway involved in VEGF-mediated HDAC7 degradation. HUVECs were pretreated for 1 hour with SU1498 (tyrosine kinase inhibitor), U73122 (PLC $\gamma$  inhibitor), R59022 (diacylglycerol kinase inhibitor), LY294002 (phosphatidylinositol 3-kinase/AKT inhibitor), PD98059 (mitogen-activated protein kinase inhibitor), and inositol-1,4,5-trisphosphate (IP3) (IP3 kinase [IP3K] inhibitor) before 20 ng/mL VEGF treatment for 10 minutes. Western blot analysis showed that both U73122 and IP3 block VEGF-induced HDAC7 protein degradation, whereas the other inhibitors had no effect (Figure 5B). Furthermore U73122 and IP3K inhibitors block VEGF-mediated suppression of HDAC7 in a dose-dependent manner (Figure 5C). These results indicate that VEGF induces HDAC7 degradation through the PLC $\gamma$ -IP3K signal pathway. Moreover VEGF-induced HDAC7 degradation was ablated by MG132 treatment (Figure 5D), suggesting that degradation of HDAC7 is mediated through the proteasome. Finally, VEGF treatment decreased HDAC7 binding to  $\beta$ -catenin, whereas the binding of 14-3-3  $\zeta$  to exogenous HDAC7, which is not fully degraded by VEGF, increased (Figure 5E).

#### HDAC7 Modulates VEGF-Mediated $\beta$ -Catenin Translocation

VEGF induced HDAC7 degradation, whereas the cellular localization of  $\beta$ -catenin was related to the HDAC7 protein level. Therefore, HDAC7 may be involved in VEGF-induced  $\beta$ -catenin translocation. To explore this, the distribution of cytoplasmic and nuclear  $\beta$ -catenin was detected after VEGF treatment and overexpression of HDAC7 by adenoviral gene transfer. As expected, 10 minutes of VEGF stimulation downregulated endogenous HDAC7 protein levels and increased the nuclear versus cytoplasmic ratio of  $\beta$ -catenin (Figure 6A [left] and 6B). To confirm this finding, we performed immunofluorescence staining to determine the nuclear localization of  $\beta$ -catenin on VEGF treatment (Figure 6D). However, when HDAC7 was overexpressed, the ratio of nuclear to cytoplasmic  $\beta$ -catenin decreased and VEGF no longer induced nuclear translocation of  $\beta$ -catenin. In fact the nuclear portion was reduced (Figure 6A [right] and 6B). Moreover in cells overexpressing HDAC7 VEGF no longer exerts a proliferative effect (Figure 6C). However, by increasing VEGF stimulation (100 ng/mL) the inhibitory effect of Ad-HD7 on  $\beta$ -catenin nuclear translocation can be partially overcome as revealed by double immunostaining experiments (Figure 6E). Interestingly, stimulation of cells overexpressing

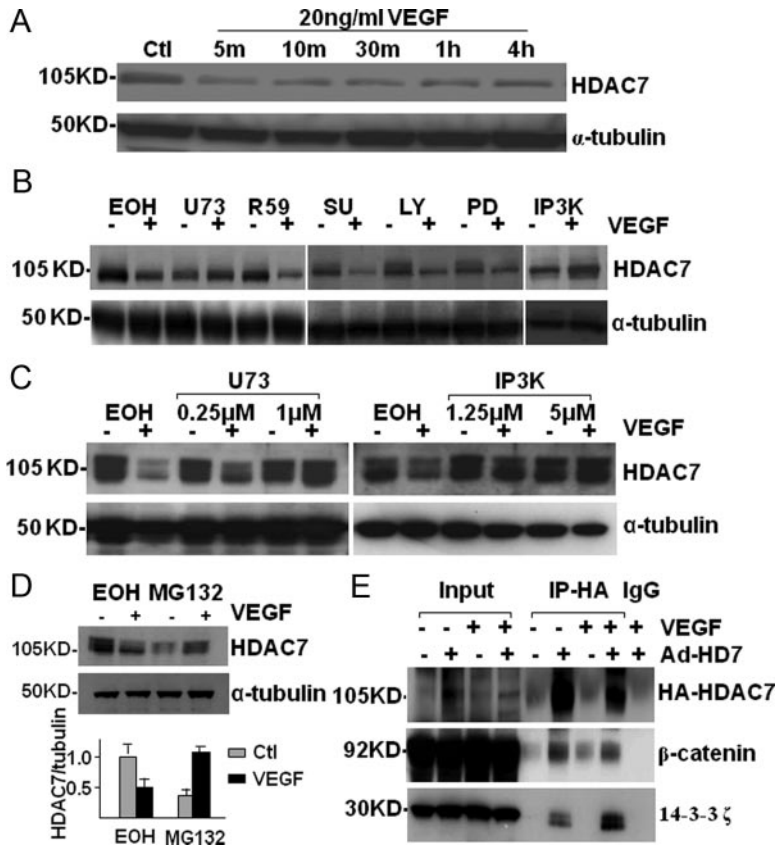


**Figure 5. VEGF induces HDAC7 protein degradation through the PLC $\gamma$ -IP3K pathway.** **A**, VEGF treatment decreases HDAC7 protein level. HUVECs were treated with VEGF (20 ng/mL) for the indicated time. HDAC7 protein level is decreased as early as 5 minutes after treatment, as revealed by Western blot analysis;  $\alpha$ -tubulin was used as a loading control. **B**, VEGF induces HDAC7 degradation through the PLC $\gamma$ -IP3K signal pathway. HUVECs were pretreated with specific inhibitors for 1 hour, followed by treatment with 20 ng/mL VEGF for 10 minutes in the presence of inhibitors. EOH indicates ethanol; U73, U73122 (PLC inhibitor); R59, R59022 (diacylglycerol kinase inhibitor); SU14, SU1498; LY29, LY294002; PD89, PD98059; IP3K (IP3K inhibitor). **C**, U73122 and IP3K inhibitors attenuate VEGF-induced HDAC7 degradation in a dose-dependent manner (U73122: 0.25 to 1  $\mu$ mol/L; IP3K: 1.25 to 5  $\mu$ mol/L). **D**, MG132 inhibitor ablates VEGF-induced HDAC7 degradation. HUVECs were pretreated with MG132 for 6 hours before VEGF treatment for 10 minutes in the presence of the inhibitor. HDAC7 protein level was detected by Western blot (**top**) and 3 independent experiments were quantified (**bottom**). **E**, VEGF decreases binding of exogenous HDAC7 to  $\beta$ -catenin but increases its binding to 14-3-3  $\zeta$  proteins. Coimmunoprecipitation experiments were performed in the absence or presence of VEGF treatment for 10 minutes. HA antibody was used to pull down exogenous HDAC7 and its associated proteins.

Ad-HD7 with Wnt3a ligand, which mediates  $\beta$ -catenin nuclear translocation,<sup>25</sup> reduced  $\beta$ -catenin nuclear translocation (Online Figure VII). These results further support the notion that HDAC7 is involved in the regulation of  $\beta$ -catenin translocation.

## Discussion

The homeostasis between histone acetylation and deacetylation modulates chromosome structure, acting as a switch for gene transcription. This activity is key in cell proliferation and survival. HDACs represent an important protein family as they control histone acetylation status<sup>26</sup> and modulate gene expression through association and dissociation of sequence-specific DNA-binding transcription factors.<sup>27</sup> In this study, we found that HDAC7 formed a complex with  $\beta$ -catenin and 14-3-3  $\epsilon$ ,  $\zeta$ , and  $\eta$  proteins. HDAC7 also modulated the cellular localization of  $\beta$ -catenin, the expression of  $\beta$ -catenin target genes and cell cycle-related genes. Elevated HDAC7 retained  $\beta$ -catenin in the cytoplasm, whereas HDAC7 deficiency increased nuclear translocation of  $\beta$ -catenin. VEGF suppressed HDAC7 transcription and induced HDAC7 degradation through the PLC $\gamma$ -IP3K pathway, resulting in nuclear translocation of  $\beta$ -catenin. Overexpression of HDAC7 ablated VEGF-induced  $\beta$ -catenin translocation and EC proliferation (Figure 7). These findings suggest that HDAC7 is crucial in the regulation of EC growth and proliferation.

HDACs are involved in cell cycle regulation through modulation of gene transcription. HDAC1 controls cell cycle progression through Rb/E2F<sup>28</sup> or p53/p21.<sup>29</sup> HDAC4 inhibits cell cycle progression, increases cell survival<sup>30</sup> and plays a

role in the repression of cardiac hypertrophy,<sup>31</sup> demonstrating its important role in the cell cycle. In our study, both overexpression and knockdown of HDAC7 downregulated cyclin D1 and caused cell cycle elongation at G1 phase, suggesting that tight regulation of the HDAC7 protein level is important for EC cycle progression. Further research is required to elucidate this important and tightly regulated process. Recently, disruption of the HDAC7 gene in mice was shown to disrupt endothelial cell-cell adhesion and to enlarge the branchial arteries.<sup>18</sup> The enlargement of the branchial arteries may imply an increase in EC number or size. Indeed, in our experiments knockdown of HDAC7 increased HUVEC size with a concomitant increase in cellular metabolism. These data suggest that HDAC7 regulates EC cycle and growth.

$\beta$ -Catenin is essential in both cell-cell adhesion and Wnt signal transduction. However the precise control over  $\beta$ -catenin targeting to cadherin adhesive complexes, or TCF-transcriptional complexes is poorly understood. The intracellular domains of VE-cadherin bind to  $\beta$ -catenin, p71, p120 and plakoglobin.<sup>32</sup> The whole complex modulates cell-to-cell communication, controls intercellular permeability and mediates the contact inhibition of cell proliferation by preventing translocation of  $\beta$ -catenin into the nucleus.<sup>32,33</sup> It is believed that participation of  $\beta$ -catenin in adhesion of Wnt signaling is dictated by the regulation of distinct molecular forms of  $\beta$ -catenin with different binding properties, rather than simple competition between cadherins and TCFs for a single constitutive form.<sup>34</sup> However, the regulation of the distinct molecular forms of  $\beta$ -catenin remains unknown.

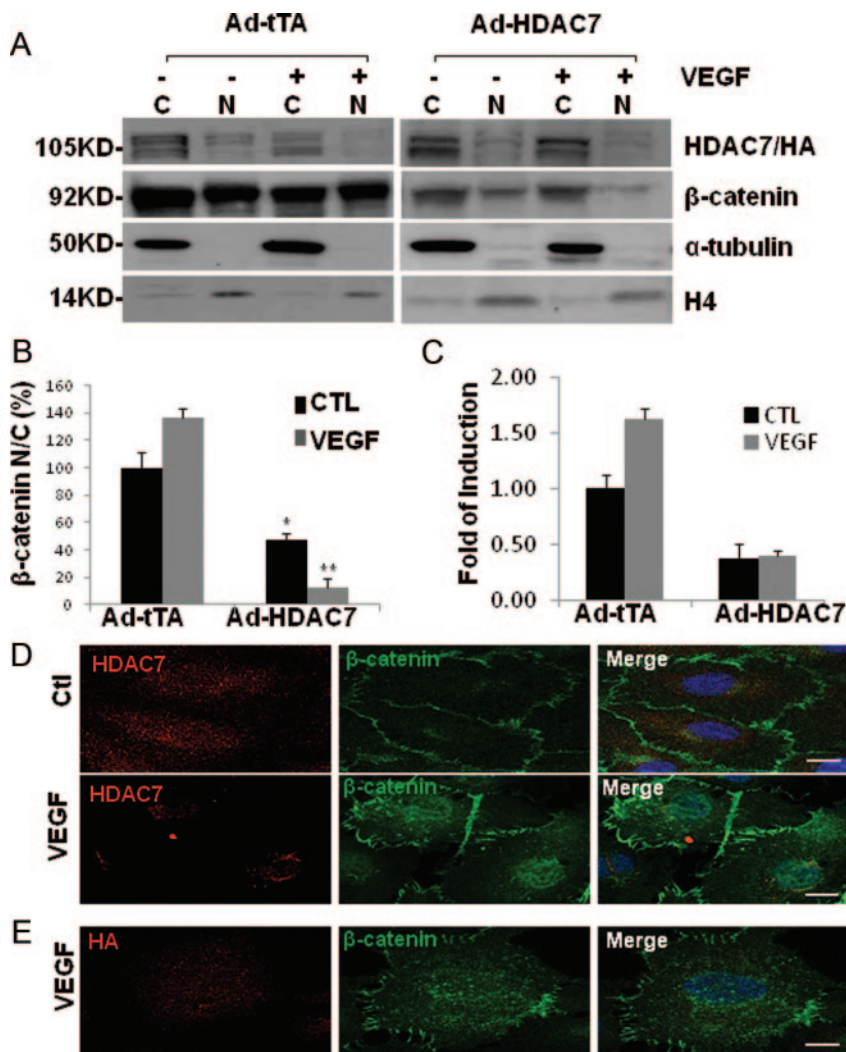


**Figure 6. HDAC7 prevents  $\beta$ -catenin translocation to the nucleus.** **A**, Overexpression of HDAC7 blocked VEGF-induced  $\beta$ -catenin translocation. HUVECs were infected for 48 hours, followed by VEGF treatment for 10 minutes. Cellular localization of HDAC7 and  $\beta$ -catenin was detected by Western blot in the cytoplasm and nuclear fractions. Endogenous and exogenous HDAC7 were detected by anti-HDAC7 and anti-HA antibodies, respectively.  $\alpha$ -Tubulin and H4 were included as loading controls for cytoplasmic and nuclear fractions, respectively. VEGF suppresses endogenous HDAC7 expression and induces nuclear localization of  $\beta$ -catenin, which is ablated by overexpression of exogenous HDAC7. The ratio of nuclear to cytoplasmic  $\beta$ -catenin in the presence of HDAC7 is decreased. **B**, Quantification and statistical analysis. \* $P < 0.05$ . **C**, Proliferation assays show that overexpression of HDAC7 ablates VEGF-induced EC proliferation. **D**, Double immunofluorescence staining confirmed the nuclear localization of  $\beta$ -catenin after VEGF treatment. **Bars**, 100  $\mu\text{m}$  and 50  $\mu\text{m}$ , respectively. **E**, Treatment with high VEGF concentration (100 ng/mL) partially overcomes the blockage of nuclear  $\beta$ -catenin by Ad-HD7 in HUVECs overexpressing Ad-HD7. **Bar**, 100  $\mu\text{m}$ .

HDAC1 and HDAC2 regulate oligodendrocyte differentiation by disrupting the  $\beta$ -catenin–TCF interaction,<sup>35</sup> which suggests that HDACs are important regulators of  $\beta$ -catenin interactions. On VEGF treatment, VEGF receptor 2 phosphorylates VE-cadherin<sup>36</sup> and  $\beta$ -catenin, leading to degradation of VE-cadherin, nuclear translocation of  $\beta$ -catenin and transcription of proliferation-related genes.<sup>37</sup> In our study, we found that overexpression of HDAC7 ablated VEGF-induced  $\beta$ -catenin translocation and EC proliferation, whereas knockdown of HDAC7 by shRNA increased  $\beta$ -catenin translocation and EC growth. Therefore, HDAC7 downregulation by VEGF plays a critical role in the stabilization of  $\beta$ -catenin in the cytoplasm.

VEGF is a growth factor and induces angiogenesis by increasing EC proliferation and migration. Several signaling pathways are activated by VEGF treatment, such as the phosphatidylinositol 3-kinase/Akt pathway that mediates cell survival,<sup>5</sup> the extracellular signal-regulated kinase/mitogen-activated protein kinase pathway that influences cell proliferation and apoptosis and the VE-cadherin/ $\beta$ -catenin/Wnt pathway that regulates cell proliferation.<sup>38,39</sup> VEGF treatment can also induce quiescent cells to re-enter the cell cycle. As the protein level of HDAC7 affects EC growth and cell cycle

progression, it is postulated that crosstalk between VEGF signaling and HDAC7 may occur and that HDAC7 is involved in VEGF-induced EC growth and proliferation. Indeed, our results showed that VEGF suppressed HDAC7 transcription and induced a rapid and transient degradation of HDAC7. Additionally, experiments performed in the presence of the proteasome inhibitor MG132 demonstrated that VEGF induced degradation of HDAC7 occurred through the proteasome. MG132 alone also degraded HDAC7, as shown previously.<sup>40</sup> Further studies revealed that the PLC $\gamma$ -IP3K signal pathway is involved in VEGF-mediated HDAC7 degradation. The transiently reduced levels of HDAC7 in response to VEGF resulted in a prompt increase in nuclear translocation of  $\beta$ -catenin and enhanced EC proliferation. In concert with this, when VEGF cannot effectively decrease exogenous HDAC7 protein following HDAC7 overexpression, it could neither increase nuclear translocation of  $\beta$ -catenin nor trigger EC proliferation. Indeed, with increasing VEGF stimulation (100 ng/mL), the blockage of nuclear  $\beta$ -catenin by HDAC7 overexpression was partially overcome, whereas stimulation of cells overexpressing HDAC7 with a wnt3a ligand reduced nuclear translocation of  $\beta$ -catenin.

The localization of HDAC7 is crucial for its function. Previous studies suggest that HDAC7 is a shuttle protein and

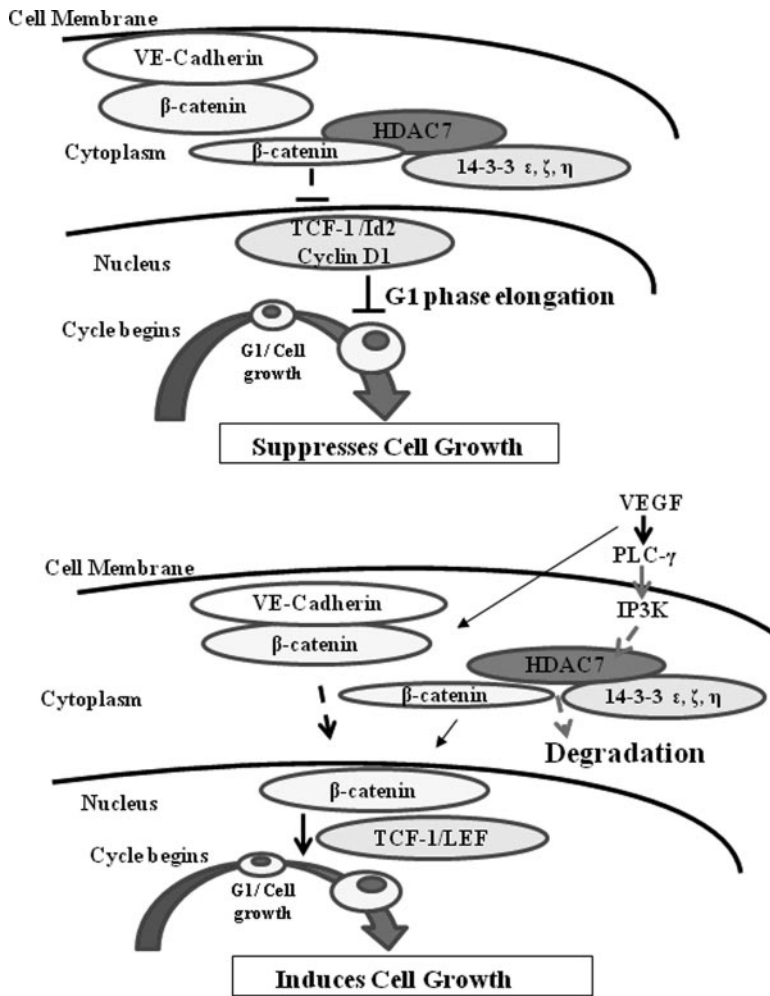


**Figure 7. A schematic illustration shows the role of HDAC7 in the control of EC growth.** HDAC7 acts as a bridge between 14-3-3  $\epsilon, \zeta, \eta$ , and  $\beta$ -catenin and stabilizes  $\beta$ -catenin in the cytoplasm, resulting in inhibition of EC growth and leading to G<sub>1</sub> phase elongation. VEGF treatment increases HDAC7 degradation, releasing  $\beta$ -catenin from the HDAC7- $\beta$ -catenin-14-3-3 complex, leading to the translocation of  $\beta$ -catenin to the nucleus. The overall effect is an increase in  $\beta$ -catenin target gene expression and EC growth.

is detected both in the cytosol and the nucleus. We found that the experimental design and culture conditions such as cell confluence, culture media, the presence or absence of growth factors (eg, VEGF, vascular endothelial cell growth factor) influenced the localization of HDAC7. Overexpression of HDAC7 could also alter its subcellular location, with lower multiplicities of infection (eg, 10 mois) resulting in cytoplasmic localization and higher multiplicities of infection (eg, 100 mois) resulting in nuclear localization. To overcome the limitations of the in vitro systems we performed an en face staining of ECs on perfused arteries obtained from wild type mice. These experiments indicated that HDAC7 protein in ECs in vivo is mainly cytoplasmic. This further supports the notion that HDAC7 translocation to the nucleus is a tightly monitored process.

The 14-3-3 proteins seem to affect HDAC7 localization by controlling the stabilization of cytoplasmic HDAC7 and protecting it from proteolysis.<sup>40,41</sup> Members of this family also form a complex with  $\beta$ -catenin and increase its steady-state levels in the cytoplasm.<sup>24</sup> Our experiments demonstrated that HDAC7 formed a complex with 14-3-3  $\epsilon, \zeta, \eta$  proteins and  $\beta$ -catenin. However, a detailed analysis of the function of the various 14-3-3 members in this complex went beyond the scope of the present work. Nevertheless, initial experiments suggested an important role for 14-3-3  $\zeta$ . It

bound directly to HDAC7 but not to  $\beta$ -catenin. This may indicate that HDAC7 functions as a scaffold that provides docking sites for 14-3-3 proteins and  $\beta$ -catenin and facilitates their binding in a stable complex. Formation of this complex stabilizes  $\beta$ -catenin in the cytoplasm. However, further experiments are needed to explore this aspect.

Phosphorylation of HDAC7 in response to VEGF stimulation adds an additional layer of regulation. VEGF stimulates PLC $\gamma$ , which activates protein kinase C, leading to HDAC7 phosphorylation and its cytoplasmic accumulation.<sup>20</sup> Moreover, VEGF-induced phosphorylation of HDAC7 influences its export from the nucleus and controls migration and proliferation in ECs.<sup>21</sup> Of note, when a mutant form of HDAC7 that cannot be phosphorylated was applied, VEGF failed to induce proliferation of ECs. In our experiments, expression of the mutant HDAC7 also severely suppressed VEGF induced proliferation but had no effect at baseline conditions. In contrast wild type HDAC7 that can be phosphorylated and localized to both the cytosol and the nucleus had an inhibitory effect on proliferation in the presence or absence of VEGF (Online Figure VIII). Because the mutated form localized to the nucleus, these experiments underline the significance of the cytoplasmic HDAC7 that exerts unique functions in the cell.

Importantly, different HDAC7 splicing isoforms have distinct cellular localizations, which may explain their different

functions.<sup>23</sup> Thus, it will be interesting to study the HDAC7 isoforms in ECs and to explore whether VEGF regulates such splicing events and modulates their functions. It seems that the localization and expression of HDAC7 could direct a number of VEGF-stimulated signaling pathways to regulate HDAC7 phosphorylation and degradation. Further studies are required to elucidate the above aspects.

In summary, this study provides evidence that HDAC7 controls EC proliferation through the modulation of  $\beta$ -catenin stabilization. HDAC7 bridges 14-3-3  $\epsilon$ ,  $\zeta$ ,  $\eta$  and  $\beta$ -catenin and stabilizes  $\beta$ -catenin in the cytoplasm, resulting in inhibition of EC growth and leading to the elongation of G<sub>1</sub> phase. VEGF-induced degradation of HDAC7 disrupts this complex and leads to the translocation of  $\beta$ -catenin to the nucleus, which induces EC growth. This study provides novel insights into the mechanisms involved in EC growth.

### Acknowledgments

We thank Dr John Paul Kirton for critical reading of the manuscript and Dr Alexander Kapustin for his kind help using the Multisizer 3 Coulter Counter (Beckman Coulter).

### Sources of Funding

British Heart Foundation and Oak Foundation.

### Disclosures

None.

### References

- Dejana E, Spagnuolo R, Bazzoni G. Interendothelial junctions and their role in the control of angiogenesis, vascular permeability and leukocyte transmigration. *Thromb Haemost*. 2001;86:308–315.
- Liebner S, Cavallaro U, Dejana E. The multiple languages of endothelial cell-to-cell communication. *Arterioscler Thromb Vasc Biol*. 2006;26:1431–1438.
- Foteinos G, Hu Y, Xiao Q, Metzler B, Xu Q. Rapid endothelial turnover in atherosclerosis-prone areas coincides with stem cell repair in apolipoprotein E-deficient mice. *Circulation*. 2008;117:1856–1863.
- Dejana E. Endothelial cell-cell junctions: happy together. *Nat Rev*. 2004;5:261–270.
- Gerber HP, McMurtrey A, Kowalski J, Yan M, Keyt BA, Dixit V, Ferrara N. Vascular endothelial growth factor regulates endothelial cell survival through the phosphatidylinositol 3'-kinase/Akt signal transduction pathway. Requirement for Flk-1/KDR activation. *J Biol Chem*. 1998;273:30336–30343.
- Lampugnani MG, Orsenigo F, Gagliani MC, Tacchetti C, Dejana E. Vascular endothelial cadherin controls VEGFR-2 internalization and signaling from intracellular compartments. *J Cell Biol*. 2006;174:593–604.
- Carmeliet P, Jain RK. Angiogenesis in cancer and other diseases. *Nature*. 2000;407:249–257.
- Claesson-Welsh L. Signal transduction by vascular endothelial growth factor receptors. *Biochem Soc Trans*. 2003;31:20–24.
- Carmeliet P. Mechanisms of angiogenesis and arteriogenesis. *Nat Med*. 2000;6:389–395.
- Gottardi CJ, Gumbiner BM. Adhesion signaling: how beta-catenin interacts with its partners. *Curr Biol*. 2001;11:R792–R794.
- Rockman SP, Currie SA, Ciavarella M, Vincan E, Dow C, Thomas RJ, Phillips WA. Id2 is a target of the beta-catenin/T cell factor pathway in colon carcinoma. *J Biol Chem*. 2001;276:45113–45119.
- Willert J, Epping M, Pollack JR, Brown PO, Nusse R. A transcriptional response to Wnt protein in human embryonic carcinoma cells. *BMC Dev Biol*. 2002;2:8.
- Taurin S, Sandbo N, Qin Y, Browning D, Dulin NO. Phosphorylation of beta-catenin by cyclic AMP-dependent protein kinase. *J Biol Chem*. 2006;281:9971–9976.
- Zeng L, Xiao Q, Margariti A, Zhang Z, Zampetaki A, Patel S, Capogrossi MC, Hu Y, Xu Q. HDAC3 is crucial in shear- and VEGF-induced stem cell differentiation toward endothelial cells. *J Cell Biol*. 2006;174:1059–1069.
- Lee JH, Hart SR, Skalnik DG. Histone deacetylase activity is required for embryonic stem cell differentiation. *Genesis*. 2004;38:32–38.
- Chang S, McKinsey TA, Zhang CL, Richardson JA, Hill JA, Olson EN. Histone deacetylases 5 and 9 govern responsiveness of the heart to a subset of stress signals and play redundant roles in heart development. *Mol Cell Biol*. 2004;24:8467–8476.
- Shin HJ, Baek KH, Jeon AH, Kim SJ, Jang KL, Sung YC, Kim CM, Lee CW. Inhibition of histone deacetylase activity increases chromosomal instability by the aberrant regulation of mitotic checkpoint activation. *Oncogene*. 2003;22:3853–3858.
- Chang S, Young BD, Li S, Qi X, Richardson JA, Olson EN. Histone deacetylase 7 maintains vascular integrity by repressing matrix metalloproteinase 10. *Cell*. 2006;126:321–334.
- Mottet D, Bellahcene A, Pirrotte S, Waltregny D, Deroanne C, Lamour V, Lidereau R, Castronovo V. Histone deacetylase 7 silencing alters endothelial cell migration, a key step in angiogenesis. *Circ Res*. 2007;101:1237–1246.
- Ha CH, Jhun BS, Kao HY, Jin ZG. VEGF stimulates HDAC7 phosphorylation and cytoplasmic accumulation modulating matrix metalloproteinase expression and angiogenesis. *Arterioscler Thromb Vasc Biol*. 2008;28:1782–1788.
- Wang S, Li X, Parra M, Verdin E, Bassel-Duby R, Olson EN. Control of endothelial cell proliferation and migration by VEGF signaling to histone deacetylase 7. *Proc Natl Acad Sci U S A*. 2008;105:7738–7743.
- Zeng L, Zampetaki A, Margariti A, Pepe AE, Alam S, Martin D, Xiao Q, Wang W, Jin ZG, Cockerill G, Mori K, Li YS, Hu Y, Chien S, Xu Q. Sustained activation of XBP1 splicing leads to endothelial apoptosis and atherosclerosis development in response to disturbed flow. *Proc Natl Acad Sci U S A*. 2009;106:8326–8331.
- Margariti A, Xiao Q, Zampetaki A, Zhang Z, Li H, Martin D, Hu Y, Zeng L, Xu Q. Splicing of HDAC7 modulates the SRF-myocardin complex during stem-cell differentiation towards smooth muscle cells. *J Cell Sci*. 2009;122:460–470.
- Tian Q, Feetham MC, Tao WA, He XC, Li L, Aebbersold R, Hood L. Proteomic analysis identifies that 14-3-3zeta interacts with beta-catenin and facilitates its activation by Akt. *Proc Natl Acad Sci U S A*. 2004;101:15370–15375.
- Oloumi A, Syam S, Dedhar S. Modulation of Wnt3a-mediated nuclear beta-catenin accumulation and activation by integrin-linked kinase in mammalian cells. *Oncogene*. 2006;25:7747–7757.
- de Ruijter AJ, van Gennip AH, Caron HN, Kemp S, van Kuilenburg AB. Histone deacetylases (HDACs): characterization of the classical HDAC family. *Biochem J*. 2003;370:737–749.
- Kuo MH, Allis CD. Roles of histone acetyltransferases and deacetylases in gene regulation. *Bioessays*. 1998;20:615–626.
- Ferreira R, Naguibneva I, Mathieu M, Ait-Si-Ali S, Robin P, Pritchard LL, Harel-Bellan A. Cell cycle-dependent recruitment of HDAC-1 correlates with deacetylation of histone H4 on an Rb-E2F target promoter. *EMBO Rep*. 2001;2:794–799.
- Zeng L, Zhang Y, Chien S, Liu X, Shyy JY. The role of p53 deacetylation in p21Waf1 regulation by laminar flow. *J Biol Chem*. 2003;278:24594–24599.
- Majdzadeh N, Wang L, Morrison BE, Bassel-Duby R, Olson EN, D'Mello SR. HDAC4 inhibits cell-cycle progression and protects neurons from cell death. *Dev Neurobiol*. 2008;68:1076–1092.
- Karamboulas C, Swedani A, Ward C, Al-Madhoun AS, Wilton S, Boisvenue S, Ridgeway AG, Skerjanc IS. HDAC activity regulates entry of mesoderm cells into the cardiac muscle lineage. *J Cell Sci*. 2006;119:4305–4314.
- Venkiteswaran K, Xiao K, Summers S, Calkins CC, Vincent PA, Pumiglia K, Kowalczyk AP. Regulation of endothelial barrier function and growth by VE-cadherin, plakoglobin, and beta-catenin. *Am J Physiol Cell Physiol*. 2002;283:C811–C821.
- Lampugnani MG, Corada M, Caveda L, Breviario F, Ayalon O, Geiger B, Dejana E. The molecular organization of endothelial cell to cell junctions: differential association of plakoglobin, beta-catenin, and alpha-catenin with vascular endothelial cadherin (VE-cadherin). *J Cell Biol*. 1995;129:203–217.
- Gottardi CJ, Gumbiner BM. Distinct molecular forms of beta-catenin are targeted to adhesive or transcriptional complexes. *J Cell Biol*. 2004;167:339–349.
- Ye F, Chen Y, Hoang T, Montgomery RL, Zhao XH, Bu H, Hu T, Taketo MM, van Es JH, Clevers H, Hsieh J, Bassel-Duby R, Olson EN, Lu QR.

- HDAC1 and HDAC2 regulate oligodendrocyte differentiation by disrupting the beta-catenin-TCF interaction. *Nat Neurosci.* 2009;12:829–838.
36. Esser S, Lampugnani MG, Corada M, Dejana E, Risau W. Vascular endothelial growth factor induces VE-cadherin tyrosine phosphorylation in endothelial cells. *J Cell Sci.* 1998;111(Pt 13):1853–1865.
  37. Wallez Y, Huber P. Endothelial adherens and tight junctions in vascular homeostasis, inflammation and angiogenesis. *Biochim Biophys Acta.* 2008;1778:794–809.
  38. Herren B, Levkau B, Raines EW, Ross R. Cleavage of beta-catenin and plakoglobin and shedding of VE-cadherin during endothelial apoptosis: evidence for a role for caspases and metalloproteinases. *Mol Biol Cell.* 1998;9:1589–1601.
  39. Masckauchan TN, Shawber CJ, Funahashi Y, Li CM, Kitajewski J. Wnt/beta-catenin signaling induces proliferation, survival and interleukin-8 in human endothelial cells. *Angiogenesis.* 2005;8:43–51.
  40. Li X, Song S, Liu Y, Ko SH, Kao HY. Phosphorylation of the histone deacetylase 7 modulates its stability and association with 14-3-3 proteins. *J Biol Chem.* 2004;279:34201–34208.
  41. Martin M, Kettmann R, Dequiedt F. Class IIa histone deacetylases: regulating the regulators. *Oncogene.* 2007;26:5450–5467.

### Novelty and Significance

#### What Is Known?

- Histone deacetylases (HDACs) are involved in cell cycle regulation.
- $\beta$ -Catenin activates cell cycle specific genes.
- Vascular endothelial growth factor (VEGF) induces angiogenesis.

#### What New Information Does This Article Contribute?

- HDAC7 directly interacts with  $\beta$ -catenin.
- HDAC7 controls endothelial cell (EC) growth through the stabilization of cytoplasmic  $\beta$ -catenin.
- VEGF induces degradation of HDAC7, which leads to nuclear  $\beta$ -catenin translocation and EC growth induction. These findings shed light on the mechanisms involved in EC growth.

ECs form cell-to-cell junctions and regulate vascular homeostasis. HDAC7, a member of the class II HDACs, is necessary for

angiogenesis. It is also known that  $\beta$ -catenin induces cell proliferation. However, the stabilization and cytoplasmic to nuclear translocation of  $\beta$ -catenin are poorly understood. The goal of this study was to examine the role of HDAC7 in EC proliferation and growth and to uncover the underlying mechanism. The most important finding is that HDAC7 directly interacts with  $\beta$ -catenin and influences its cellular localization. Interestingly, increased levels of HDAC7 maintain  $\beta$ -catenin in the cytoplasm. This work demonstrates for the first time that HDAC7 is crucial in  $\beta$ -catenin cytoplasmic stabilization and in the control of EC growth. These findings are important for future research on the regulation of EC proliferation and growth and for understanding the mechanisms of endothelial integrity in the vasculature.

## I Text

### Supplemental Methods and Material

#### Materials

Antibodies [goat anti-HDAC7 (C-18, sc-11491), rabbit anti-14-3-3  $\zeta$  (C-16, sc-1019), goat anti-14-3-3  $\eta$  (E-12, sc-17287) and 14-3-3  $\epsilon$  (E-20, sc-31962), rabbit anti-Histone H4 (H-97, sc-10810), mouse anti-VE-cadherin (F-8, sc-9989) rabbit anti- $\beta$ -catenin (H102, sc-7199)], mouse anti-Cyclin D1 (A-12, sc-8396), mouse anti-E2F2 (TFE-25, sc-9967), rabbit anti-Rb (C-15, sc-50), rabbit anti-caspase-2 (H-19, sc-623), rabbit anti-caspase-3 (H-277, sc-7148), and mouse anti-caspase-9 (4i31, sc-70507) were purchased from Santa Cruz Biotech (Santa Cruz, CA, USA); Antibodies [mouse anti- $\alpha$ -tubulin (Clone B-5-1-2, T 5168), rabbit-anti-HDAC7 (KG-17, H 2662), mouse anti-HA (Clone HA-7, H9658), and monoclonal anti-HA agarose-conjugated antibody (A2095) ] were from Sigma (St Louis, MO, USA). Anti-Active- $\beta$ -Catenin [anti-ABC, clone 8E7 (05-665)] was from Millipore. Mouse anti-HDAC7 (ab50212) was purchased from Abcam. All secondary antibodies were from Dakocytomation (Glostrup, Denmark). Recombinant Human VEGF 165 (293-VE), and Wnt-3a (5036-WN) were purchased from R & D Systems. The Topflash reporter plasmid was from Millipore (21-170).

#### Cell culture

Human umbilical vein endothelial cells (HUVECs) were isolated from the human umbilical cord and cultured on collagen I-coated flasks in EGM-2 medium (Clonetics) or in M199 medium supplemented with 1ng/ml  $\beta$ -endothelial cell growth factor (SIGMA), 3  $\mu$ g/ml EC Growth Supplement from bovine neural tissue (SIGMA), 10U/ml heparin, 1.25 $\mu$ g/ml thymidine, 5% foetal bovine serum (FBS, PAA, A15-108)<sup>1</sup>, 100 $\mu$ g/ml penicillin and streptomycin in a humidified incubator supplemented with 5% CO<sub>2</sub>. With both media, similar results have been obtained. The cells were subcultured every three days at a ratio of 1:4. Cells up to passage 8 were used in this study. 293T cells were maintained in DMEM supplemented with 10% FBS and penicillin/streptomycin. Living cell images were assessed by Nikon Eclipse TS100 microscope with Ph1 ADL 10x/0.25 objective lenses and Nikon DS-Fil camera at room temperature and processed by Adobe Photoshop software.

#### Plasmid and Ad-virus construction

The expression vector pShuttle2-HDAC7 (HD7) and corresponding Ad-HDAC7 viral DNA (Ad-HD7) was constructed as described previously<sup>2</sup>. All plasmids were verified by DNA sequencing. The mutant HDAC7 plasmid was a kind gift from Professor Eric N. Olson (University of Texas Southwestern Medical Center).

#### RNA extraction and reverse transcriptase-polymerase chain reaction (RT-PCR) and Real-time PCR

RT-PCR and Real time PCR were performed as described previously<sup>2</sup>. Total RNA was extracted using the RNeasy Mini Kit (Qiagen) according to the manufacturer's protocol. 2  $\mu$ g RNA were reversely transcribed into cDNA with random primer by MMLV reverse transcriptase (RT) (Promega). 20-50ng cDNA (relative to RNA amount) was amplified by standard PCR with *Taq* DNA polymerase (Invitrogen) or real time PCR. Primers for HDAC7 and  $\beta$ -actin have been described previously<sup>2</sup>, primers for other HDACs and cell cycle related genes are shown in

supplementary table I. PCR primers for real time PCR were designed using Primer Express software (Applied Biosystems).

### **Immunoblotting**

Cells were harvested and washed with cold PBS, resuspended in lysis buffer (25mM Tris-Cl pH 7.5, 120mM NaCl, 1 mM EDTA pH 8.0, 0.5% Triton X100) supplemented with protease inhibitors (Roche) and lysed by ultrasonication (twice, 6 seconds each) (Bradson Sonifier150) for whole cell lysate, or with Hypotonic buffer (10 mM HEPES-KOH pH 7.2, 1.5 mM MgCl<sub>2</sub>, 10 mM KCl, 0.5% NP-40 ) and High-salt buffer (20 mM HEPES-KOH pH 7.2, 25% Glycerol, 1.5 mM MgCl<sub>2</sub>, 420 mM KCl, 0.2 mM EDTA) supplemented with protease inhibitors for cytoplasmic and nuclear fractions. The protein concentration was determined using the Biorad Protein Assay Reagent. 50µg of whole lysate or nuclear and cytoplasmic fractions was applied to SDS-PAGE and transferred to Hybond PVDF membrane (GE Health), followed by standard western blot procedure. The bound primary antibodies were detected by the use of horseradish peroxidase (HRP)-conjugated secondary antibody and the ECL detection system (GE Health). The band density was semi-quantified by Adobe Photoshop software.

### **Indirect immunofluorescence Assay (IIFA)**

HUVECs were seeded on collagen I-coated slides, and HDAC7 was overexpressed by adenoviral gene transfer or suppressed by HDAC7 shRNA lentiviral plasmid transfer (NM\_019572 SIGMA). Staining was also performed for the endogenous HDAC7 in HUVECs as described previously<sup>2</sup>. Briefly, the cells were fixed with 4% paraformaldehyde and permeabilised with 0.1% Triton X-100 in PBS for 10 min and blocked in 5% swine serum in PBS for 30 min at 37°C. Incubation with the primary antibodies, HDAC7 (goat), β-catenin (rabbit), and HA (mouse) was performed for 1 h at 37 °C. The bound primary antibodies were revealed by incubation with an ALEXA 546 conjugated donkey anti-goat IgG, and a FITC-conjugated swine anti-rabbit IgG, or FITC-conjugated anti-mouse IgG at 37°C for 30 min. Cells were counterstained with 4', 6-diamidino-2-phenylindole (DAPI; Sigma) and mounted in Floromount-G (DAKOCytomation, Glostrup, Denmark) and examined with SP5 confocal microscope (Leica, Germany). Magnification is indicated as scale bar in Figures.

### ***En face* staining**

All animal experiments were performed according to protocols approved by the Institutional Committee for Use and Care of Laboratory Animals. For *en face* staining preparations using double immunofluorescence, the thoracic artery was harvested from mice and cut into 2 mm<sup>2</sup> segments. The tissue was fixed with 4% paraformaldehyde. The aortic segments were then pinned on a silicon base, permeabilised with 0.1% Triton X-100 in PBS for 40 min and blocked in 10% swine serum in PBS for 1h at 37°C. Incubation with the primary antibodies, HDAC7 (goat, Santa Cruz and CD31 (ab7388, rat) was performed overnight at 4°C. The bound primary antibodies were detected by incubation with an ALEXA 546 conjugated donkey anti-goat IgG and a FITC-conjugated swine anti-rat IgG at 37°C for 2h. The tissue was counterstained with 4', 6-diamidino-2-phenylindole (DAPI; Sigma) and mounted on microscope slides in Floromount-

G (DAKOCytomation, Glostrup, Denmark) and examined with SP5 confocal microscope (Leica, Germany). Magnification is indicated as scale bar in figures.

### **Adenoviral gene transfer**

For adenoviral gene transfer HUVECs were seeded on collagen I-coated dishes 24h prior to infection. Infection was performed for 12 h and fresh medium was added to the cells. Ad-tTA virus (Tetracycline-controlled transactivator tTA adenovirus, commercially available) was included as control and to compensate for the MOI.

### **Lentiviral particle transduction**

Lentiviral particles were produced using MISSION shHDAC7 plasmids DNA (SIGMA) according to protocol provided. The shRNA Non-Targeting vector was used as a negative control. Briefly, 293T cells were transfected with the lentiviral vector and the packaging plasmids, pCMV-dR8.2 and pCMV-VSV-G (both obtained from Addgene) using Fugene 6. The supernatant containing the lentivirus was harvested 48h later, filtered, aliquoted and stored at  $-80^{\circ}\text{C}$ . p24 antigen ELISA (Zeptometrix) was used to determine the viral titre. The Transducing Unit (TU) was calculated using the conversion factor recommended by the manufacturer ( $10^4$  physical particles per pg of p24 and 1 transducing unit per 103 physical particles for a VSV-G pseudotyped lentiviral vector), with 1pg of p24 antigen converted to 10 Transducing Units (TU). For lentiviral infection, HUVECs were seeded overnight on collagen I-coated plates or flasks. The next day cells were incubated with shHDAC7 or Non Targeting control ( $1 \times 10^7$  TU/ml) in complete medium supplemented with  $10 \mu\text{g/ml}$  of Polybrene for 24h. Subsequently, fresh medium was added to the cells and the plates were returned to the incubator and harvested 48h later and subjected to further analysis.

### **Proliferation Assay**

HUVECs were infected with lentiviral shRNA or Ad-HD7 and Ad-tTA. A sample of uninfected cells was used as a control. Twenty four hours later, the cells were sub-cultured into 24-well plate at  $3 \times 10^4$  cells/well with medium refreshed next day. Cell proliferation assay was performed 72h after infection with CellTiter 96 AQueous One Solution Cell Proliferation Assay kit (Promega, Cat No. G3580) according to the protocol provided. The fold of induction was defined as the A490nm of test group to that of the control group with that of control set as 1.0

### **BrdU incorporation**

HUVECs were seeded in 6-well plate at  $1.5 \times 10^5$  cells/well 24h prior to infection. Twenty four hours after the lentiviral shRNA or Adenoviral infection, the viral particles were removed and fresh medium was added to the cells. Forty-eight hours after infection, the cells were dispensed with trypsin and counted, followed by re-plating in two 24-well plates at  $1 \times 10^4$  cells/well, 3 wells in each plate for each group. The remaining cells were re-plated in fresh 6 well plates. Six hours later, cells in one 24-well plate was labeled with BrdU for 18h. Twenty-four hours after trypsinization, the BrdU labeled cells were subjected to BrdU incorporation assay (5-Bromo-2'-deoxy-Uridine Labeling and Detection Kit III, Ref 11444611001, Roche) according to protocol provided. Cells in the other 24-well plate were subjected to proliferation assay as described above. Cells in 6-well plates were subjected to western blot to detect knockdown efficiency. All assays were performed at 72hours after infection. The fold of induction for BrdU incorporation was defined as the ratio of A405nm for BrdU incorporation assay to A490nm for proliferation assay with that of control group set as 1.0.

### **FACS Analysis**

Forty-eight hours post infection of HUVECs with Ad-HD7 or Ad-tTA, the cells were harvested by incubating cell cultures with dissociation buffer (GIBCO). The harvested cells were fixed in 70% ethanol for at least 30 minutes and washed twice in PBS. Fixed cells were incubated with PBS containing propidium iodide (PI) and RNase at 37°C for 45 minutes, and analysed with a FACS scan flow cytometer (Becton Dickinson Immunocytometry Systems, Mountain View, CA, USA). Forward and 90° side scatter were used to identify cell population and single cell fractions were gated out to perform further analysis of PI staining intensity. Data analysis was carried out using CellQuest software (Becton Dickinson).

### **Cell size calculation and cell count**

For calculation of the cell size and cell count, HUVECS were infected with lentiviral shRNA or Ad-HD7 or mutant HDAC7 and control viruses (control non-infected cells and the infected ones with non-targeting ShRNA lentivirus, and Ad-tTA, respectively). Twenty four, 48 and 72 hours after infection the cells were trypsinized and subjected to cell size calculation using a multisizer 3 coulter counter (Beckman Coulter), according to the manufacturer's instructions.

### **Co-immunoprecipitation**

HUVECs were infected with Ad-HD7 for 12h, followed by further incubation with growth medium for 36h. The cells were lysed by 1h rotation at 4°C in lysis buffer (25mM Tris-Cl pH 7.5, 150mM NaCl, 1 mM EDTA pH 8.0, 0.5% Triton X100) supplemented with protease inhibitors. One milligram of whole lysate was subjected to standard co-immunoprecipitation procedure. Briefly, lysates were pre-cleared with normal IgG and then incubated with HA (Sigma) or  $\beta$ -catenin or HDAC7 or 14-3-3  $\zeta$  antibodies for 2h at 4°C and precipitated by overnight incubation with protein-G/beads. Precipitated proteins were resolved by SDS gel electrophoresis and subsequently immunoblotted with HA, HDAC7,  $\beta$ -catenin, VE-Cadherin and 14-3-3 antibodies, or mass spectrometry analysis was performed.

### **Mass spectrometry**

SDS-PAGE gels were silver stained<sup>3</sup> and protein bands showing differential expression between the Ad-HD7-infected and the control groups (Ad-tTA) were excised. After tryptic digestion, peptides were lyophilized and resuspended in 0.05% TFA<sup>4</sup>. Peptides were eluted through Acclaim C18 PepMap100 column (P/N 164261, Dionex) with acetonitrile gradient from 4% to 25% in 35min and detected by an LTQ Orbitrap XL (Thermo Scientific) mass analyser using dynamic exclusion. Spectra were searched against UniProt/SPROT database using SEQUEST program (Bioworks Browser version 3.3.1, Thermo Scientific). The result files were imported into Scaffold software (version 2.0, Proteome Software) and protein identifications were exported using the following filter: peptide probability >95.0%, protein probability >99.0%, a minimum of 2 unique peptides and a mass accuracy < 10 parts per million (www.vascular-proteomics.com).

### **VEGF and Wnt3a treatment**

For VEGF treatment, HUVECs were seeded on collagen I coated plates / flasks for 24h cultured with complete media (M199 plus supplements or EGM-2). For short term VEGF treatment (5-30 minutes) the cells were cultured in the absence of serum from 6-24 hours prior to VEGF treatment. For long term VEGF treatment (24h), the cells were cultured in the absence of serum for 2-6 hours, prior to VEGF treatment. During VEGF treatment no serum was included in the media. For the inhibitor experiments, HUVECs were pre-treated with inhibitors for 1 h. SU1493, U73122, LY294002, PD98059 and IP3 inhibitors (purchased from CALBIOCHEM) were dissolved in DMSO or ethanol, and used at the indicated concentrations (SU1493, U73122,

R59022, Ly294002, PD98059: 1 $\mu$ M, and IP3 (Cat. No. 406170) inhibitors: 5 $\mu$ M. The U73122 and IP3K inhibitors were tested in a dose dependent manner U73122: 0.25 $\mu$ M - 1 $\mu$ M, IP3K: 1.25  $\mu$ M - 5 $\mu$ M. The cells were cultured for 2h in the absence of serum, and then pre-treated with a specific inhibitor for 1h or 6h for MG132 before VEGF (20ng/ml) treatment in the presence of the inhibitor. For Wnt-3a stimulation, HUVECs were infected with Ad-tTA or Ad-HD7 and 48 hours later the cells were stimulated with 100ng/ml of Wnt3a for 6 hours in EBM-2 plus 0.5% FBS. Cells were lysed and subjected to immunoblotting procedures or fixed and immunostained.

#### **Annexin V staining**

Annexin V staining was performed using the Annexin V-FITC BMS306F1; Bender MedSystems, according to manufacturer's recommendations. Briefly, HUVECs infected with Ad-HD7 (MOI:10), Ad-tTA control virus, or uninfected were trypsinized, washed with PBS and incubated with Annexin V for 10 min at room temperature. The staining was analysed with a FACS scan flow cytometer (Becton Dickinson Immunocytometry Systems, Mountain View, CA, USA).

#### **Luciferase Activity Assay**

For transient transfection, HUVECs were seeded on collagen I-coated 12-well plate at  $2.5 \times 10^4$  cells/well 24h prior to transfection with pGL3-Luc-HDAC7 reporter gene<sup>2</sup>, or TOPFLASH reporter gene (0.33 $\mu$ g/well) using Fugene-6-Reagent (Roche Molecular Biochemicals), according to the manufacturer's instructions, and treated with VEGF (20ng/ml) for 24h. Renilla-Luc (0.1 $\mu$ g/well) was included in all transfection assays as an internal control. Forty-eight hours later, firefly and renilla luciferase activity was assessed with respective assay kit (Promega). The relative luciferase activity (RLU) was defined as the ratio of readout for firefly luciferase to that for renilla luciferase with that of control group set as 1.0.

#### **Statistical analysis**

Data expressed as the means $\pm$ SEM were analysed with a two-tailed student's *t*-test for two-groups or pair-wise comparisons. A value of  $p < 0.05$  was considered to be significant.

## References

1. Zeng L, Zampetaki A, Margariti A, Pepe AE, Alam S, Martin D, Xiao Q, Wang W, Jin ZG, Cockerill G, Mori K, Li YS, Hu Y, Chien S, Xu Q. Sustained activation of XBP1 splicing leads to endothelial apoptosis and atherosclerosis development in response to disturbed flow. *Proc Natl Acad Sci U S A*. 2009;106:8326-8331.
2. Margariti A, Xiao Q, Zampetaki A, Zhang Z, Li H, Martin D, Hu Y, Zeng L, Xu Q. Splicing of HDAC7 modulates the SRF-myocardin complex during stem-cell differentiation towards smooth muscle cells. *J Cell Sci*. 2009;122:460-470.
3. Yan JX, Wait R, Berkelman T, Harry RA, Westbrook JA, Wheeler CH, Dunn MJ. A modified silver staining protocol for visualization of proteins compatible with matrix-assisted laser desorption/ionization and electrospray ionization-mass spectrometry. *Electrophoresis*. 2000;21:3666-3672.
4. Sidibe A, Yin X, Tarelli E, Xiao Q, Zampetaki A, Xu Q, Mayr M. Integrated membrane protein analysis of mature and embryonic stem cell-derived smooth muscle cells using a novel combination of CyDye/biotin labeling. *Mol Cell Proteomics*. 2007;6:1788-1797.

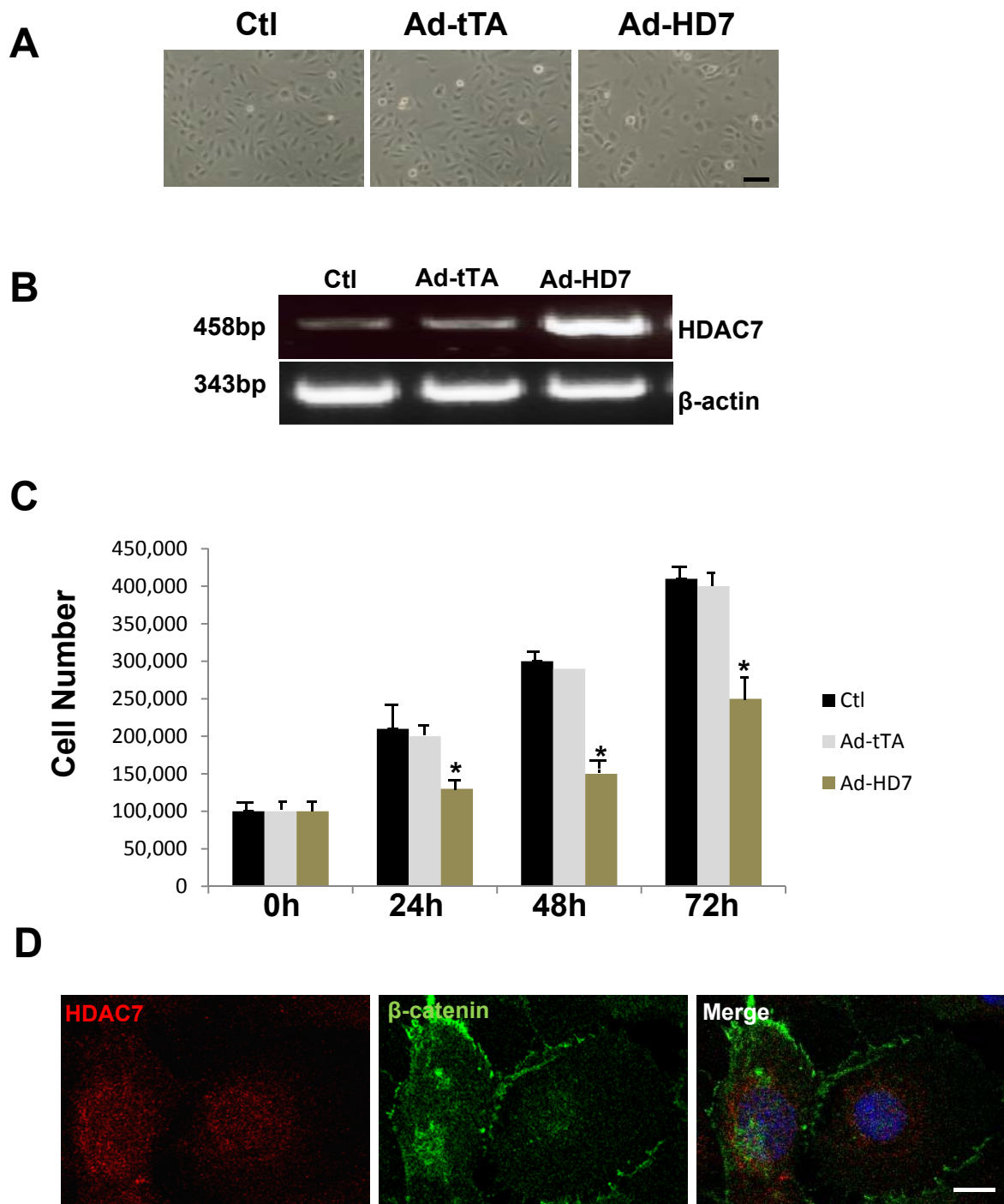


**Figure I: Elevated HDAC7 suppresses EC proliferation.**

(A) HUVECs were uninfected (Ctl) or infected with Ad-HD7 or Ad-tTA. The cell morphology was observed. Bar: 50  $\mu$ m. (B) HDAC7 expression was detected at 48h post-infection by PCR. (C) HUVECs were uninfected (Ctl) or infected with Ad-HD7 or Ad-tTA. 12 h later (it was defined as 0h) the cells were subcultured and 100,00 cells from each group were seeded on a 6 well plate and cell counts were performed at 24h, 48h and 72h thereafter, \* $p < 0.05$ . (D) Double Immunofluorescence staining for HDAC7 and  $\beta$ -catenin in control uninfected cell under subconfluent conditions. Junctional and nuclear  $\beta$ -catenin localisation were observed, (bar: 100  $\mu$ m). The data presented were representative or means $\pm$ SEM of three independent experiments.

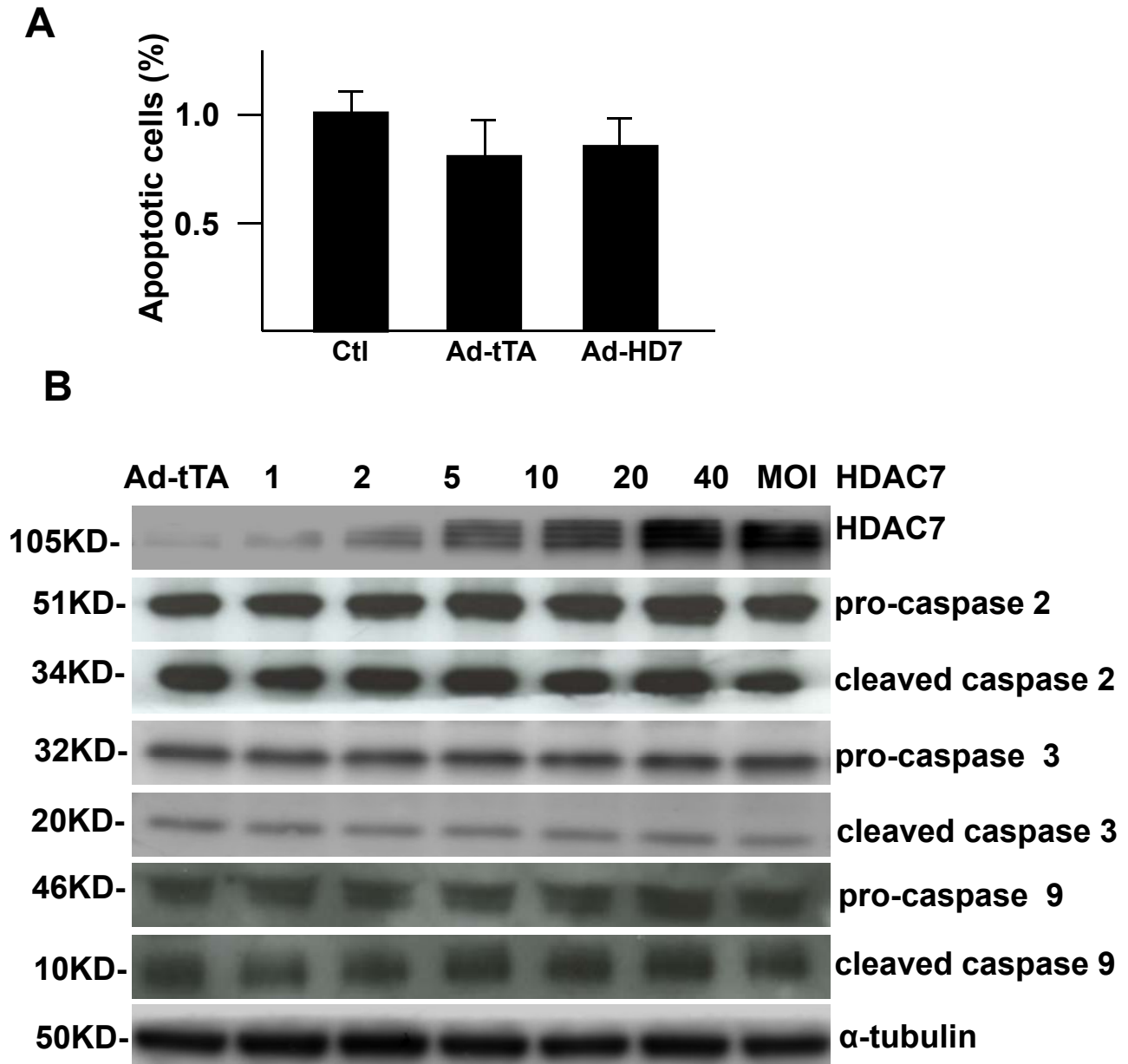


**Figure II: HDAC7 does not induce apoptosis in ECs**

(A) HUVECs were infected with Ad-HD7 (MOI: 10), Ad-tTA control virus, or uninfected cells and Annexin V staining was performed in order to detect apoptosis. The staining was analysed with a FACS scan flow cytometer. (B) Western blot showed that overexpression of HDAC7 does not induce caspase activation. HUVECs were infected with Ad-HD7 (MOI: 1-40), Ad-tTA was used as a control virus and also to compensate for the total amount of virus. Forty eight hours post infection, the cells were harvested and total protein was extracted. Caspase 2, 3 and 9 activation was detected by Western blot.  $\alpha$ -tubulin was used as a loading control. No caspase activation was changed. The data shown are representative of two independent experiments.

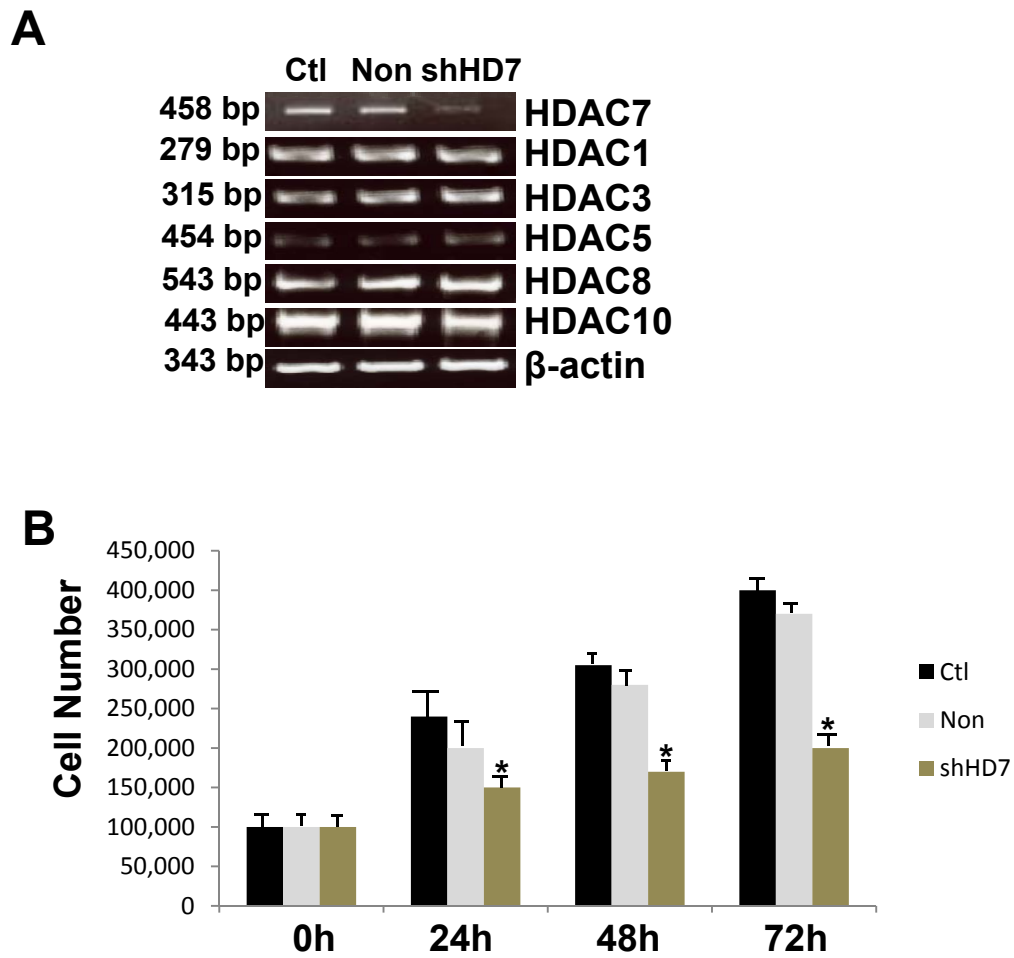


**Figure III: Knockdown of HDAC7 suppresses the cell count**

(A) HUVECs were uninfected (Ctl) or infected with non-target (Non) or HDAC7 (shHD7) shRNA lentiviral particles, and the expression level of HDAC7 and other HDACs was tested by RT-PCR at 72h post-infection. β-actin was included as loading control. HDAC7 shRNA knocked down HDAC7 mRNA without affecting the expression of other HDACs. (B) HUVECs were uninfected (Ctl) or infected with non-target (Non) or HDAC7 (shHD7) shRNA lentiviral particles. 12 h later (it was defined as 0h) the cells were subcultured and 100,00 cells from each group were seeded on a 6 well plate and cell counts were performed at 24h, 48h and 72h thereafter, \*p<0.05. The data presented are representative or means±SEM of three independent experiments.

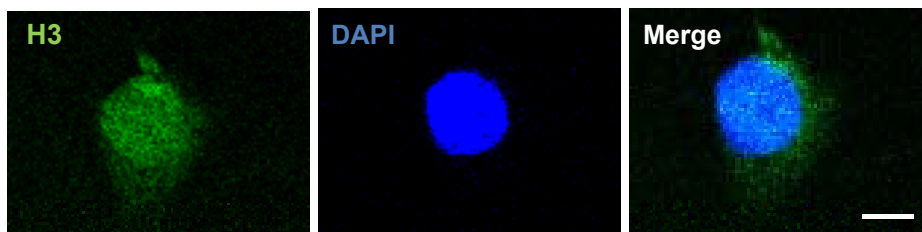


**Figure IV: H3 Nuclear Staining.**

H3 was used as a positive control for nuclear staining in HUVECs. (Bars: 50  $\mu$ m). The data presented are representative of two independent experiments.

Figure V

Margariti et al

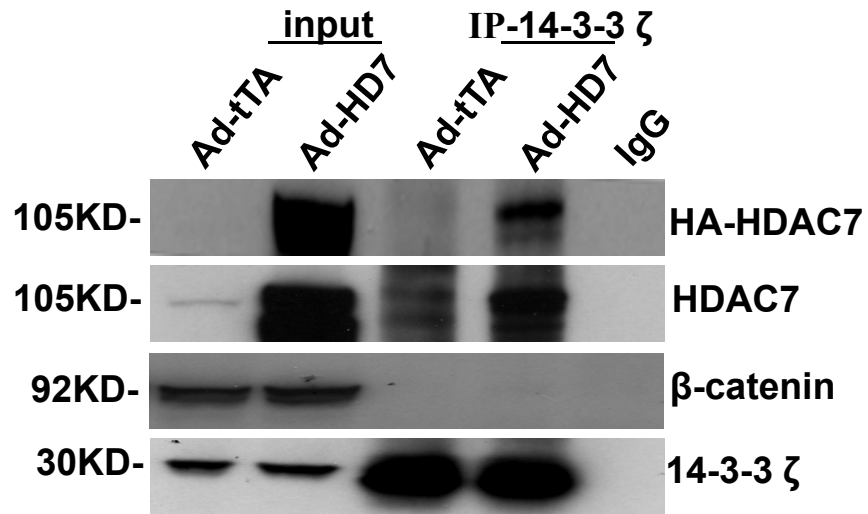
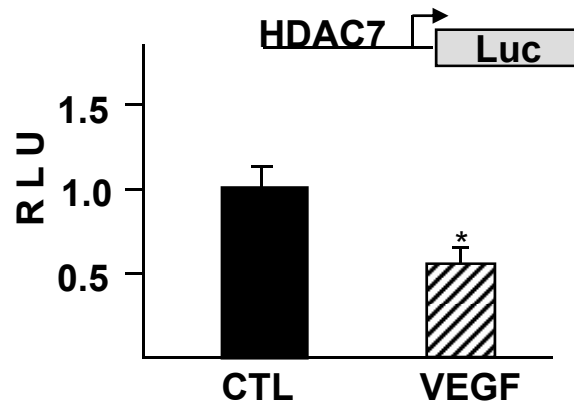


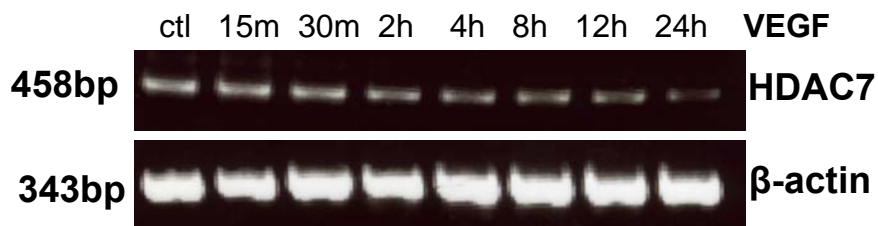
**Figure V: 14-3-3 ζ directly interacts with HDAC7, but not with β-catenin.**

Co-immunoprecipitation experiments have been performed with the 14-3-3 ζ antibody in HUVECs over-expressing HA-tagged HDAC7. The binding with native HDAC7, HA tag and β-catenin were tested.

**A**



**B**



**C**

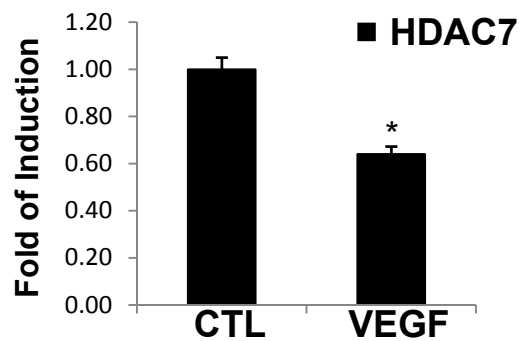


**Figure VI: VEGF treatment suppresses HDAC7 transcription.**

(A) Luciferase reporter assays show that VEGF decreases HDAC7 transcription. HUVECs were transfected with HDAC7 promoter luciferase reporter gene and treated with VEGF (20 ng/ml) for 24 hours, followed by luciferase activity assay. Renilla-luciferase reporter was included as internal control. \* $p < 0.05$ . (B) Routine RT-PCR reveals that VEGF decreased HDAC7 mRNA level.  $\beta$ -actin is used as a loading control. (C) VEGF suppresses HDAC7 expression at the RNA level tested by real-time PCR after 24h VEGF treatment. The data shown are representative of three independent experiments.

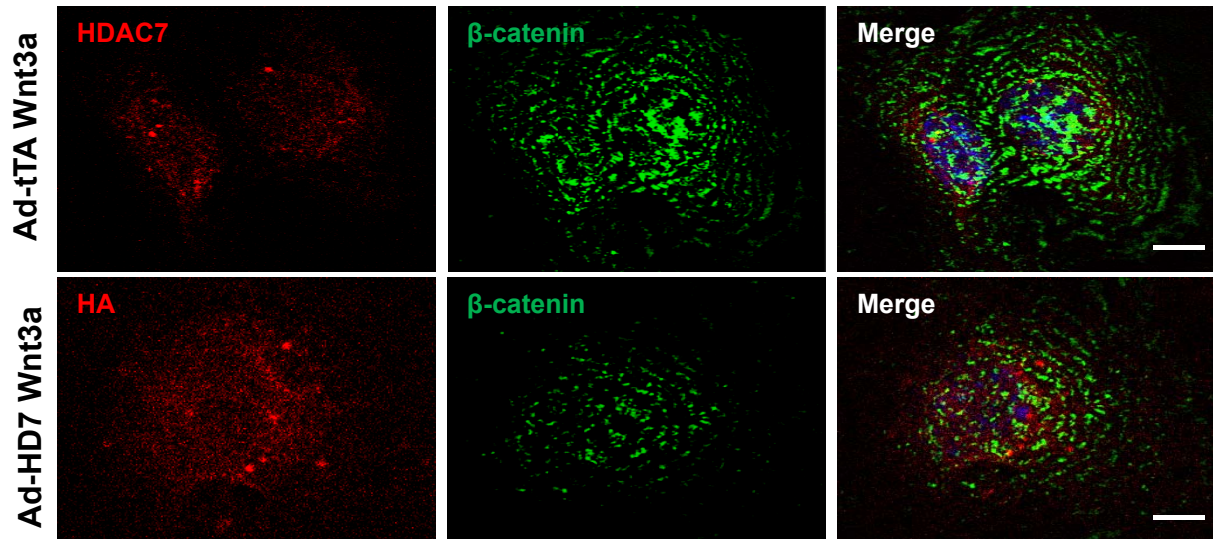


**Figure VII: Reduced  $\beta$ -catenin nuclear translocation is observed upon Wnt3a stimulation in HUVECs over-expressing Ad-HD7.** HUVECs infected with Ad-tTA or Ad-HD7 and stimulated with Wnt3a ligand and the  $\beta$ -catenin nuclear translocation was observed by double Immunofluorescence staining. Bars 100 $\mu$ m. The data shown are representative of two independent experiments.

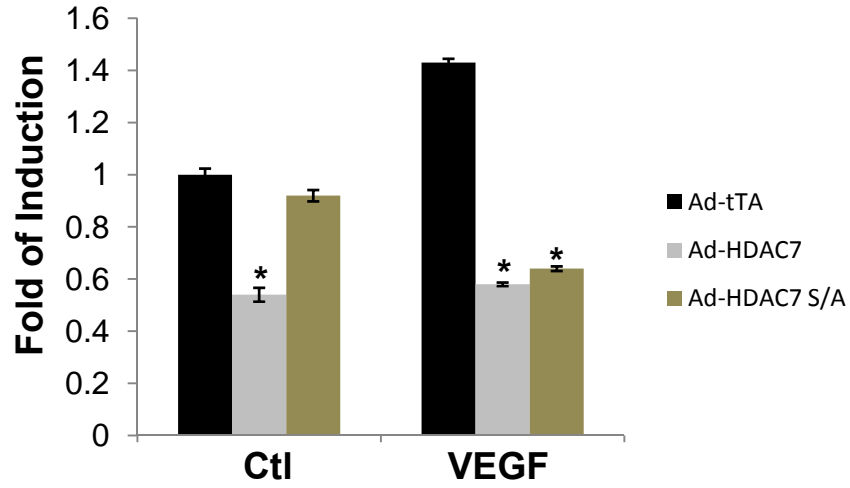


**Figure VIII: Mutant versus wild type HDAC7 on EC proliferation**

The mutant HDAC7, which is localised to the nucleus and is unable to be phosphorylated and translocated to the cytoplasm was compared with wild type HDAC7 on EC proliferation. Cell counts reveal that the mutant HDAC7 ablates EC proliferation only in response to VEGF. However, the wild type HDAC7 suppresses EC proliferation with or without VEGF stimulation. The data presented were representative of four independent experiments.

**Table I: PCR primers**

<b>Gene</b>	<b>Primers</b>	<b>Acc No.</b>
<b>HDAC1</b>	5'-GCTCAACTATGGTCTCTACC-3' 5'-CAGTTCACAGCGATGTCCGTC-3'	(NM_004964, NM_008228)
<b>HDAC3</b>	5'-CATCTCTGCTGGTAGAAGAGG-3' 5'-CATCATAGAACTCATTGGGTG-3'	(NM_010411, NM_003833)
<b>HDAC5</b>	5'-CTCTACACGTCTCCTTCTCTG-3' 5'-GCATGACCAGCTGCTGCAGG-3'	(NM_005474, BC060609)
<b>HDAC8</b>	5'-ATCTCAATGATGCTGTCTGG-3' 5'-CATGATCTGGGATCTCAGAGG-3'	(NM_018486, BC061257)
<b>HDAC10</b>	5'-TGGCACCGCTATGAGCATGG-3' 5'-CTCTAGGGCACTCTGACATGG-3'	(NM_032019, BC064018)
<b>Id2</b>	5'-GACTACATCTTGGACCTGCAG-3' 5'-GCTTATTCAGCCACACAGTGC-3'	(NM_002166)
<b>TCF-1</b>	5'-TCAATCTGCTCATGCATTACC-3' 5'-AGGTCAGGGAGTAGAAGCCAG-3'	X59870
<b>HDAC7</b>	5'-CCCAGTGTGC TCTACATTTCCC-3' 5' CACGTTGACATTGAAGCCCTC-3'	(AF207749)
<b>β-catenin</b>	5'- GCTGCTGTTTTGTTCCGAATGT-3' 5'- GCCATTGGCTCTGTTCTGA AGA-3'	(NM_001098209)
<b>LEF1</b>	5'- AGAGAAAGGAGCAGGAGCCAAA-3' 5'- ACACTCAGCAACGACATTCGC-3'	(NM_001130713)
<b>TCF3-TV1</b>	5'- CTCGGTCATCCT GAACTTGGAG-3' 5'- CCACACCTGACACCTTTTCCTC-3'	(NM_003200)
<b>Cyclin D1</b>	5'- CCC GCACGATTCATTGAAC-3' 5'- GCGGATTGGAAATGAACTTCAC-3'	(BC000076)
<b>Cyclin E1</b>	5'- GAAGGCCCTTAAGTGGCGTTT-3' 5'- TGCGGCAGTAGCACTTCATGT-3'	(NM_001238)
<b>E2F2</b>	5'- GGCGCATCTATGACATCACCA-3' 5'- GGTCTCAAACATTCCTC TGC-3'	(NM_004091)
<b>Axin 2</b>	5'>AGTGTGAGGTCCACG GAAAC<3' 5'>TGGTGCAAAGACATAGCCAG<3'	(NM_004655)

**Table II: Detailed information for the peptides of the proteins identified after IP for HA from Ad-HDAC7 compared to Ad-tTA control virus-infected HUVECs**

Sample	Protein name	accession number	Mw (Da)	Probability	Unique peptides	Unique spectra	Total spectra	Sequence coverage
A	14-3-3 protein zeta/delta	1433Z_HUMAN	27,727.90	100.00%	4	4	7	20.00%
		Position	Peptide sequence	Xcorr	DCn	+2H	+3H	Calculated MH+ Mass (AMU)
		12-27	LAEQAERYDDMAACMK	4.63	0.479	0	2	1,933.81
		28-41	SVTEQGAELSNEER	5.05	0.528	1	0	1,548.71
		42-49	NLLSVAYK	2.63	0.133	2	0	907.53
		128-138	YLAEVAAGDDK	3.54	0.470	2	0	1,151.56
Sample	Protein name	accession number	Mw (Da)	Probability	Unique peptides	Unique spectra	Total spectra	Sequence coverage
A	14-3-3 protein gamma	1433G_HUMAN	28,285.10	100.00%	4	4	7	19.40%
		Position	Peptide sequence	Xcorr	DCn	+2H	+3H	Calculated MH+ Mass (AMU)
		13-28	LAEQAERYDDMAAAMK	4.65	0.132	0	2	1,844.82
		29-42	NVTELNEPLSNEER	5.01	0.636	2	0	1,643.79
		43-50	NLLSVAYK	2.63	0.133	2	0	907.53
		133-142	YLAEVATGEK	3.15	0.367	1	0	1,080.56
Sample	Protein name	accession number	Mw (Da)	Probability	Unique peptides	Unique spectra	Total spectra	Sequence coverage
A	14-3-3 protein eta	1433F_HUMAN	28,201.60	99.00%	3	3	5	13.80%
		Position	Peptide sequence	Xcorr	DCn	+2H	+3H	Calculated MH+ Mass (AMU)
		29-42	AVTELNEPLSNEDR	5.03	0.378	2	0	1,586.77
		43-50	NLLSVAYK	2.63	0.133	2	0	907.53
		144-155	NSVVEASEAAYK	4.15	0.524	1	0	1,267.62
Sample	Protein name	accession number	Mw (Da)	Probability	Unique peptides	Unique spectra	Total spectra	Sequence coverage
A	Heat shock protein beta-1	HSPB1_HUMAN	22,764.60	99.90%	3	3	3	8.78%
		Position	Peptide sequence	Xcorr	DCn	+2H	+3H	Calculated MH+ Mass (AMU)
		5-12	RVPFLLR	2.25	0.188	1	0	987.61
		6-12	VPFLLR	2.26	0.126	1	0	831.51
		80-89	QLSSGVSEIR	2.15	0.141	1	0	1,075.57
Sample	Protein name	accession number	Mw (Da)	Probability	Unique peptides	Unique spectra	Total spectra	Sequence coverage
B	14-3-3 protein zeta/delta	1433Z_HUMAN	27,727.90	100.00%	4	4	5	20.00%
		Position	Peptide sequence	Xcorr	DCn	+2H	+3H	Calculated MH+ Mass (AMU)
		12-27	LAEQAERYDDMAACMK	4.46	0.438	0	1	1,933.81

		28-41	SVTEQGAELSNEER	5.17	0.516	1	0	1,548.71
		42-49	NLLSVAYK	2.82	0.248	1	0	907.53
		128-138	YLAEVAAGDDK	3.69	0.448	2	0	1,151.56
Sample	Protein name	accession number	Mw (Da)	Probability	Unique peptides	Unique spectra	Total spectra	Sequence coverage
B	14-3-3 protein gamma	1433G_HUMAN	28,285.10	100.00%	4	4	5	19.40%
		Position	Peptide sequence	Xcorr	DCn	+2H	+3H	Calculated MH+ Mass (AMU)
		13-28	LAEQAERYDDMAAAMK	5.33	0.103	0	1	1,844.82
		29-42	NVTELNEPLSNEER	4.93	0.653	1	0	1,643.79
		43-50	NLLSVAYK	2.82	0.248	1	0	907.53
		133-142	YLAEVATGEK	3.59	0.381	2	0	1,080.56
Sample	Protein name	accession number	Mw (Da)	Probability	Unique peptides	Unique spectra	Total spectra	Sequence coverage
B	Heat shock protein beta-1	HSPB1_HUMAN	22,764.60	99.60%	2	2	2	8.29%
		Position	Peptide sequence	Xcorr	DCn	+2H	+3H	Calculated MH+ Mass (AMU)
		6-12	VPFLLR	1.92	0.300	1	0	831.51
		80-89	QLSSGVSEIR	2.24	0.146	1	0	1,075.57
Sample	Protein name	accession number	Mw (Da)	Probability	Unique peptides	Unique spectra	Total spectra	Sequence coverage
B	14-3-3 protein eta	1433F_HUMAN	28,201.60	99.80%	3	3	5	13.80%
		Position	Peptide sequence	Xcorr	DCn	+2H	+3H	Calculated MH+ Mass (AMU)
		29-42	AVTELNEPLSNEDR	4.57	0.432	2	0	1,586.77
		43-50	NLLSVAYK	2.82	0.248	1	0	907.53
		144-155	NSVVEASEAAYK	4.25	0.586	2	0	1,267.62
Sample	Protein name	accession number	Mw (Da)	Probability	Unique peptides	Unique spectra	Total spectra	Sequence coverage
C	ADP/ATP translocase 2	ADT2_HUMAN	32,878.50	99.80%	2	2	2	5.37%
		Position	Peptide sequence	Xcorr	DCn	+2H	+3H	Calculated MH+ Mass (AMU)
		73-80	GNLANVIR	2.46	0.224	1	0	856.50
		273-280	GAWSNVLR	2.42	0.103	1	0	902.48
Sample	Protein name	accession number	Mw (Da)	Probability	Unique peptides	Unique spectra	Total spectra	Sequence coverage
C	14-3-3 protein zeta/delta	1433Z_HUMAN	27,727.90	100.00%	2	2	3	10.20%
		Position	Peptide sequence	Xcorr	DCn	+2H	+3H	Calculated MH+ Mass (AMU)
		28-41	SVTEQGAELSNEER	4.93	0.516	1	0	1,548.71
		128-138	YLAEVAAGDDK	3.49	0.468	2	0	1,151.56
Sample	Protein name	accession number	Mw (Da)	Probability	Unique peptides	Unique spectra	Total spectra	Sequence coverage
C	14-3-3 protein gamma	1433G_HUMAN	28,285.10	100.00%	3	3	4	16.20%
		Position	Peptide sequence	Xcorr	DCn	+2H	+3H	Calculated MH+ Mass (AMU)
		13-28	LAEQAERYDDMAAAMK	5.33	0.124	0	1	1,844.82

		29-42	NVTELNEPLSNEER	4.74	0.599	2	0	1,643.79
		133-142	YLAEVATGEK	3.44	0.327	1	0	1,080.56
Sample	Protein name	accession number	Mw (Da)	Probability	Unique peptides	Unique spectra	Total spectra	Sequence coverage
C	14-3-3 protein eta	1433F_HUMAN	28,201.60	99.70%	3	3	4	13.80%
		Position	Peptide sequence	Xcorr	DCn	+2H	+3H	Calculated MH+ Mass (AMU)
		29-42	AVTELNEPLSNEDR	5.15	0.352	2	0	1,586.77
		43-50	NLLSVAYK	1.9	0.247	1	0	907.53
		144-155	NSVVEASEAAYK	4.16	0.527	1	0	1,267.62
Sample	Protein name	accession number	Mw (Da)	Probability	Unique peptides	Unique spectra	Total spectra	Sequence coverage
D	14-3-3 protein epsilon	1433E_HUMAN	29,157.00	100.00%	6	6	7	21.60%
		Position	Peptide sequence	Xcorr	DCn	+2H	+3H	Calculated MH+ Mass (AMU)
		30-42	VAGMDVELTVEER	4.36	0.546	1	0	1,463.71
		43-50	NLLSVAYK	2.71	0.188	1	0	907.53
		131-141	YLAEFATGNDR	3.53	0.540	1	0	1,256.59
		131-142	YLAEFATGNDRK	3.26	0.445	1	0	1,384.69
		143-153	EAAENSLVAYK	3.09	0.455	2	0	1,194.60
		245-255	EALQDVEDENQ	3.43	0.358	1	0	1,289.55
Sample	Protein name	accession number	Mw (Da)	Probability	Unique peptides	Unique spectra	Total spectra	Sequence coverage
D	14-3-3 protein gamma	1433G_HUMAN	28,285.10	100.00%	4	4	7	19.40%
		Position	Peptide sequence	Xcorr	DCn	+2H	+3H	Calculated MH+ Mass (AMU)
		13-28	LAEQAERYDDMAAMK	4.91	0.118	0	2	1,844.82
		29-42	NVTELNEPLSNEER	4.78	0.623	2	0	1,643.79
		43-50	NLLSVAYK	2.71	0.188	1	0	907.53
		133-142	YLAEVATGEK	3.13	0.371	2	0	1,080.56